Methylcelluloses End-Functionalized with Peptides as Thermoresponsive Supramolecular Hydrogelators

Ryo Suhara[†], Mao Yamagami[†], Hiroshi Kamitakahara*[†], Arata Yoshinaga[†], Yoshimasa Tanaka[§], Toshiyuki Takano[†]

[†]*Graduate School of Agriculture, Kyoto University, Kitashirakawa-Oiwake-cho, Sakyo-ku, Kyoto 606-8502, Japan*

[§]*Center for Bioinformatics and Molecular Medicine, Graduate School of Biomedical Sciences, Nagasaki University, 1-12-4 Sakamoto, Nagasaki 852-8523, Japan*

AUTHOR INFORMATION

Corresponding Author: Hiroshi Kamitakahara

*E-mail: hkamitan@kais.kyoto-u.ac.jp; Tel: +81-75-753-6257

ORCID: Hiroshi Kamitakahara: 0000-0002-0130-1919

Abstract This paper describes the synthesis of methylcelluloses end-functionalized with peptides and an investigation into their functions. We found that aqueous solutions of methylcellulose end-functionalized not only with carbohydrates but also with peptide segments, such as di(arginine) and di(glutamic acid), behave as thermoresponsive supramolecular hydrogelators at human-body temperature. The slow drug release from thermoresponsive hydrogels of methylcelluloses end-functionalized with peptides is attributed to ionic interactions between model drugs and peptide segments in these hydrogels. Reactions of methylated cellobiose with di(arginine) and di(glutamic acid) were used to determine optimum reaction conditions for the synthesis of methylcelluloses end-functionalized with these peptide residues). The surface activities, zeta potentials, thermal properties, hydrogelation behavior, and cytotoxicities of these peptide-functionalized methylcelluloses are also discussed.

Highlights:

- Methylcelluloses end-functionalized with peptides were synthesized.
- Peptides-end-functionalized methylcelluloses behave as thermoresponsive supramolecular hydrogelators at human-body temperature.
- The slow drug release from thermoresponsive hydrogels of methylcelluloses end-functionalized with peptides was achieved.

Graphical Abstract:

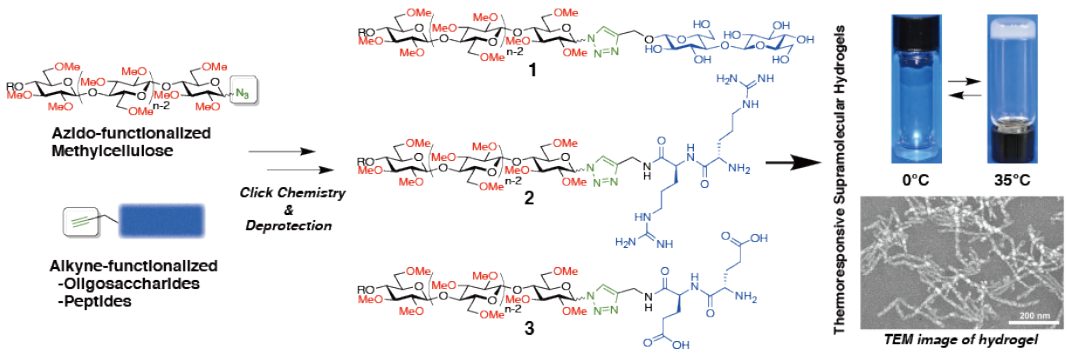

Introduction

Thermoresponsive hydrogels have received increased attention in recent years. In particular, thermoresponsive supramolecular hydrogels (Du et al. 2015) with lower critical solution temperatures (LCSTs) (Yamagami et al. 2018) enable the development of biomedical applications such as injectable drug-delivery technology (Baumann et al. 2009). While poly(*N*-isopropylacrylamide) (Fundueanu et al. 2009) is a well known thermoresponsive polymer derived from fossil resources, methylcellulose (MC) is a thermoresponsive material from renewable resources.

The degree of substitution (DS) of industrially produced MC is 1.8, and its aqueous solution exhibits thermoreversible hydrogelation at approximately 60 °C. The physical properties of aqueous MC solutions have received considerable academic attention (Desbrieres et al. 1998; Heymann 1935; Rees 1972; Savage 1957). Kato et al. concluded that the network junction points in MC gels are between 4 and 8 units long (Kato et al. 1978).

Our studies have focused on structure-property-function relationships of methylcellulose (Kamitakahara et al. 2009a; Kamitakahara et al. 2009b; Kamitakahara et al. 2008a; Kamitakahara et al. 2012; Kamitakahara and Nakatsubo 2010; Kamitakahara et al. 2006; Kamitakahara et al. 2007; Kamitakahara et al. 2009c; Kamitakahara et al. 2008b; Karakawa et al. 2002; Nakagawa et al. 2011a; Nakagawa et al. 2011b; Nakagawa et al. 2012a; Nakagawa et al. 2012b; Nakagawa et al. 2012c). Diblock methylcellulose bearing a sequence of at least ten 2,3,6-tri-*O*-methylglucosyl units and an unmodified cellobiosyl unit plays a crucial role in the thermoreversible hydrogelation of an aqueous MC solution (Nakagawa et al. 2011a).

Our detailed study on the structure-property relationships of methylcellulose with a sequence of over twenty 2,3,6-tri-*O*-methylglucosyl units revealed the thermoreversible hydrogelation properties of an aqueous diblock methylcellulose solution at human-body temperature (Nakagawa et al. 2011a). In addition, Bodvik et al. reported that MC forms fibrillar aggregates that were observed by cryogenic transmission electron microscopy (Cryo-TEM) (Bodvik et al. 2010); we also reported the same morphology (Nakagawa et al. 2012c), as did the group of Lodge (Lott et al. 2013a; Lott et al. 2013b). Moreover, we found that well-defined diblock methylcellulose self-assembles thermoresponsively into ribbon-like nanostructures in water to form a thermoreversible hydrogel at human-body temperature (Nakagawa et al. 2012c). The intermolecular interactions in the fibrillar nanostructure of commercial MC in aqueous solution at LCST and in the ribbon-like nanostructure of well-defined diblock methylcellulose are essentially the same; hydrophobic interactions between a sequence of 2,3,6-tri-*O*-methylglucosyl units, and hydrogen bonding between less-methylated glucosyl units both play crucial roles during the aggregation of methylcellulose molecules at LCST.

This finding prompted us to explore methylcellulose analogues that can be synthesized by more simple and straightforward methods than glycosylation (Nakagawa et al. 2011b). We selected the Huisgen 1,3-dipolar cycloaddition reaction for the development of methylcellulose analogues (Nakagawa et al. 2012b). An aqueous solution of the newly synthesized methylcellulose analogue, which included hydrophobic and hydrophilic segments connected by 1,2,3-triazoles, exhibited thermoreversible hydrogelation properties (Nakagawa et al. 2012b) equivalent to that of a well-defined diblock methylcellulose (Nakagawa et al. 2011b). Consequently, we developed a synthetic method for the end-

functionalization of methylcellulose to produce methylcellulosyl azide and propargyl methylcelluloside (Kamitakahara et al. 2016). Moreover, not only did nonionic segments, such as cellobiosyl units (as hydrophilic blocks) induce thermoreversible hydrogelation, but ionic segments did as well (Yamagami et al. 2018), although it was crucial that the concentrations of the diblock methylcellulose analogues in aqueous media remain at 4 wt%.

Our recent results suggested that it might be possible to install any functional group at the methylcellulose end and retain thermoreversible hydrogelation behavior at human-body temperature. Hence, we explored the end-functionalization of methylcellulose with peptides. Peptides exhibit potent biological activities due to the functional diversity of their amino-acid chains, and play crucial roles in organisms that differ from those of oligo- and polysaccharides. Therefore, the end-functionalizations of polysaccharide derivatives with peptides are expected to yield a variety of functional materials that exhibit thermoresponsive properties. An oligosaccharide-based synthetic glycoprotein (Bonduelle and Lecommandoux 2013) has been reported by the group of Lecommandoux. However, polysaccharide-derivative-*block*-oligosaccharides (Breitenbach et al. 2017; de Medeiros Modolon et al. 2012) or polysaccharide-derivative-*block*-oligopeptides have not received much attention from researchers. Carbohydrate-based block copolymers with polyester (Fajardo et al. 2014; Liu and Zhang 2007), poly(methyl methacrylate) (Dax et al. 2013; Togashi et al. 2014), poly(styrene) (Loos and Müller 2002; Otsuka et al. 2013; Yagi et al. 2010), poly(*N*-isopropylacrylamide) (Dax et al. 2013; Otsuka et al. 2012), poly(γ-benzyl-L-glutamate) (Kamitakahara et al. 2014), and poly(3-hexylthiophene) (Sakai-Otsuka et al. 2017) polyisoprene (Hung et al. 2017), and poly(ethyleneoxide) (Akiyoshi et al. 1999) have been reported. Shoichet and her

colleagues focused on a physical blend of hyaluronan and methylcellulose covalently linked to peptides for tissue-engineering purposes (Parker et al. 2016). They modified methylcellulose with peptides by the "grafting to" method, in which peptide moieties were randomly introduced onto the methylcellulose backbone. In contrast, our method gives thermoresponsive hydrogels composed of only methylcellulose and peptides, and are devoid of other polysaccharides. Our new peptide-end-functionalized methylcelluloses are linear polysaccharide derivatives with blocky structures that exhibit a broad range of new properties, including thermoreversible hydrogelation at temperatures close to that of the human body, formation of ribbonlike supramolecular nanostructures by self-assembly, surface activities, and slow drug release from thermoresponsive supramolecular hydrogel.

Herein, we describe the end-functionalization of tri-*O*-methylcellulose with cationic di(arginine) and anionic di(glutamic acid) units as peptide segments in order to develop new functionality (Chart 1). The synthesis, characterization, and thermal properties of aqueous solutions of these materials, as well as their zeta potentials, surface activities, in vitro cytotoxicities, and drug-release behavior from their supramolecular hydrogel matrices, are discussed.

Chart 1. Compounds **1**–**3**.

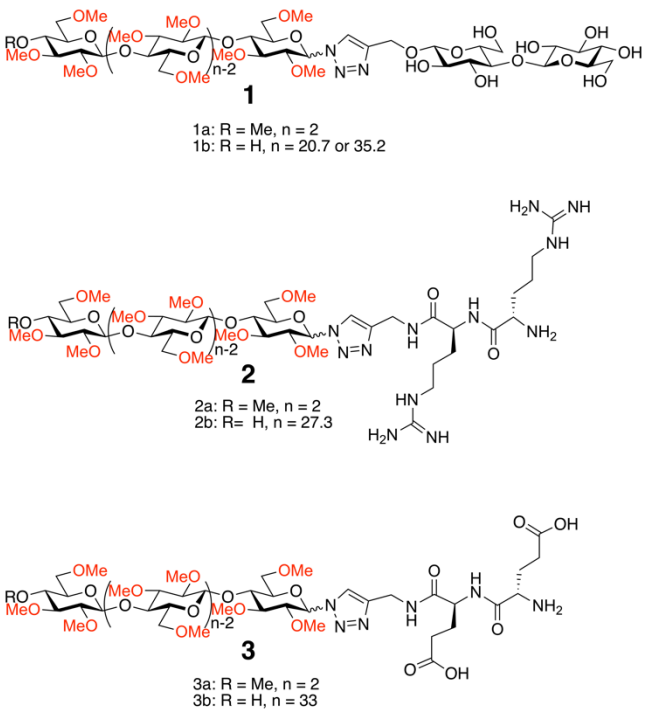

Results and discussion

Synthesis of Peptide Segments

Peptide segments were synthesized following standard Fmoc methodology, as shown in Scheme 1. For side-chain protection, we used the 2,2,4,6,7-pentamethyldihydrobenzofuran-5-sulfonyl (pbf) group for the guanidine group, while the γ carboxylic acid group of glutamic acid was protected as a *tert*-butyl (*t*Bu) ester.

Propargylamine was reacted with *N*α-Fmoc-*N*ω-Pbf-L-arginine (**11**) to give the alkyne-functionalized *N*α-Fmoc-*N*ω-Pbf-L-arginine-*N*-propargylamide (**12**) in 89% yield. The amide bond was successfully formed with DMT-MM (Kunishima et al. 1999a; Kunishima et al. 1999b) as the condensation reagent. The Fmoc group of compound **12** was removed to afford *N*ω-Pbf-L-arginine-*N*-

propargylamide (**13**) in 82% yield. *N*α-Fmoc-*N*ω-Pbf-L-arginine (**11**) was coupled with *N*ω-Pbf-L-arginine-*N*-propargylamide (**13**) to produce *N*α-Fmoc-*N*ω-Pbf-L-arginine-*N*ω-Pbf-L-arginine-*N*-propargylamide (**9**) in 89% yield.

Fmoc-Glu(O*t*-Bu)-OH (**14**) was also reacted with propargylamine to produce the alkyne-functionalized Fmoc-Glu(O*t*-Bu)-*N*-propargylamide (**15**) in quantitative yield. Removal of the Fmoc group from compound **15** afforded Glu(O*t*-Bu)-*N*-propargylamide (**16**) in quantitative yield. Compounds **14** and **16** were coupled with DMT-MM to produce *N*α-Fmoc-Glu(O*t*-Bu)-Glu(O*t*-Bu)-*N*-propargylamide (**10**) in 95% yield.

Compounds **9** and **10**, bearing alkyne groups, are peptide-containing segments for the end-functionalization of methylcellulose.

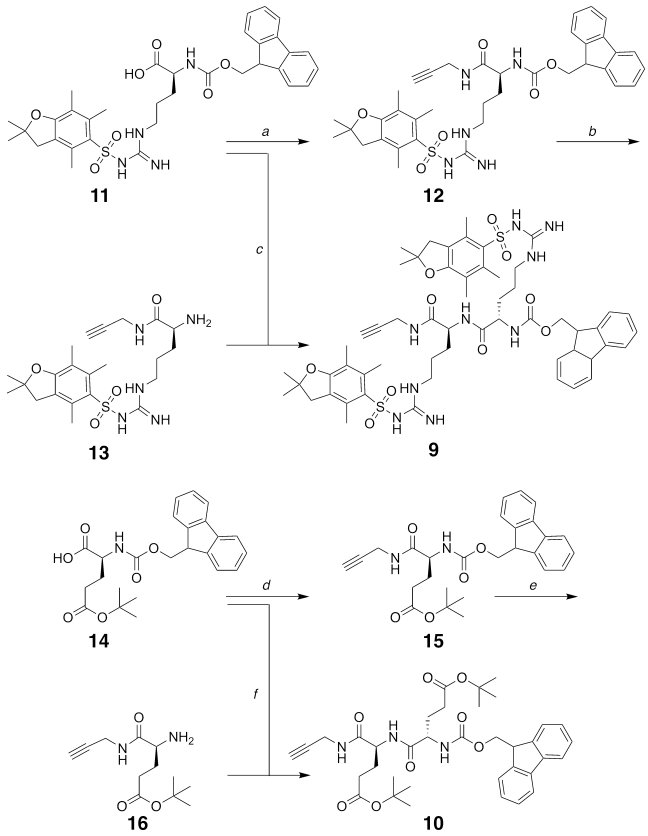

Scheme 1. Synthesis of peptide segments **9** and **10**. (a) propargylamine / DMT-MM / MeOH /r.t. / 3 h / 89%; (b) piperidine/CH_2Cl_2 / r.t. / 1 / 82%; (c) DMT-MM / MeOH / r.t. / 4 h / 89%; (d) propargylamine / DMT-MM / MeOH / r.t. 3 h / quantitative yield; (e) piperidine/CH_2Cl_2 / r.t. / 1 h / quantitative yield; (f) DMT-MM / MeOH / r.t. / 1 h / 95%.

Peptide-End-Functionalized Methylcelluloses by Huisgen 1,3-Dipolar Cycloadditions

Scheme 2 displays the synthetic routes to methylcelluloses end-functionalized with peptides, as well as the control compounds. Trehalose-type methylated cellobiose derivative **1a** and diblock methylcellulose analogues **1b** (Yamagami et al. 2018) are control compounds for peptide-functionalized methylated cellobiose derivatives **2a** and **3a**, and peptide-end-functionalized methylcelluloses **2b** and **3b**, respectively.

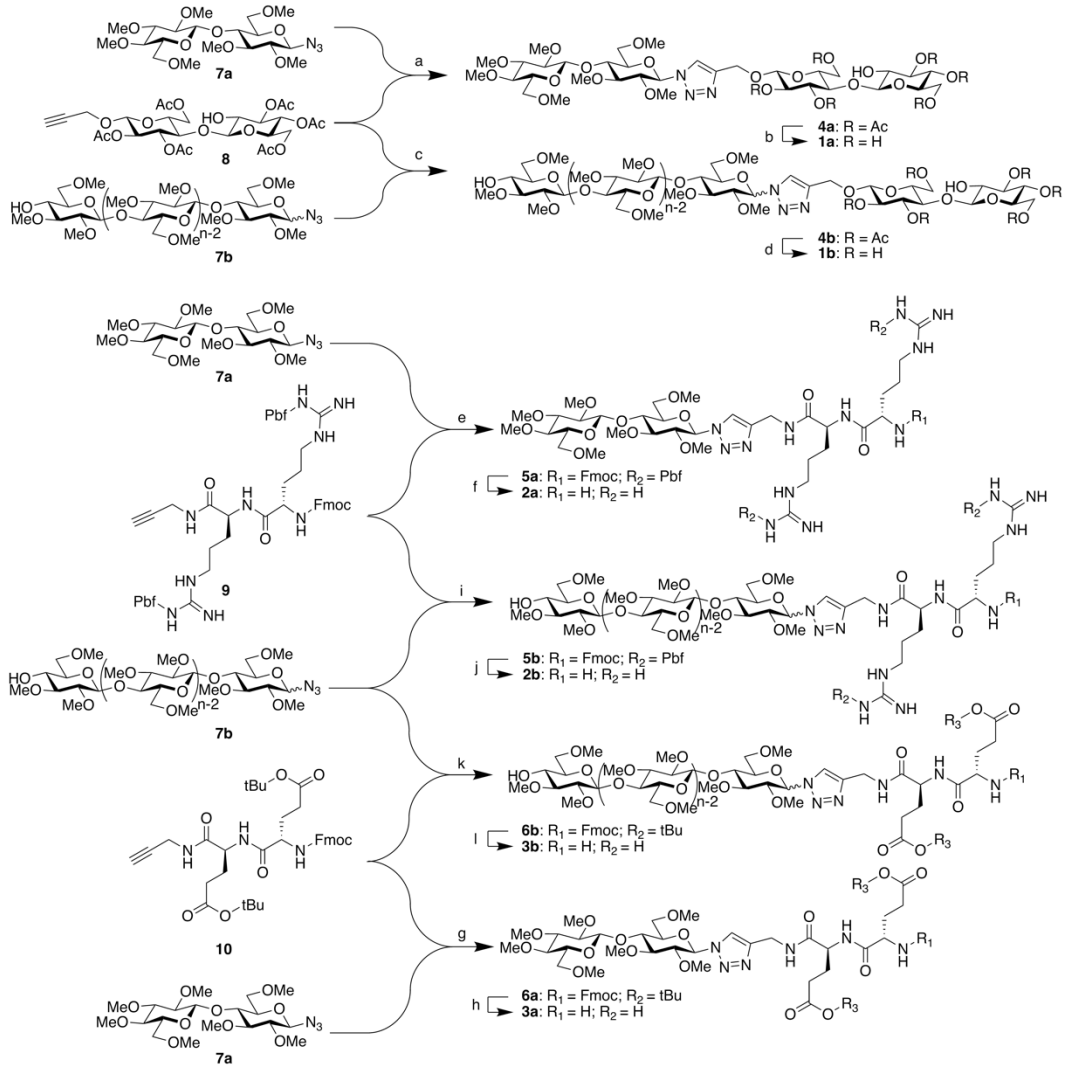

Scheme 2. Synthesis of methylcelluloses end-functionalized with peptides

a) Cu(I)Br / sodium ascorbate / PMDETA / DMF / r.t. / 21 h / 56%; b) 28% $NaOCH_3$ in MeOH / MeOH/THF / r.t. / 3 h / quantitative yield; c) CuBr / sodium ascorbate / PMDETA / MeOH/CH_2Cl_2/ r.t. / 4 d / 78.5%; d) 28% $NaOCH_3$ in MeOH / MeOH/THF / r.t. / overnight / quantitative yield; e) Cu(I)Br / sodium ascorbate / MeOH/CH_2Cl_2/ r.t. / 2 h/ 85%; f) piperidine /

CH_2Cl_2 / r.t. / 1 h / 65%; TFA/H_2O /37 °C / 4 h / 52%; g) CuBr / sodium ascorbate / MeOH / CH_2Cl_2 / r.t. / 2 h / 87%; h) piperidine / CH_2Cl_2 / r.t. / 1 h / 47%; TFA/H_2O/ r.t. / 4 h / 58%; i) $CuSO_4 \cdot H_2O$ / sodium ascorbate / MeOH/CH_2Cl_2 / r.t. / 14 h/ quantitative yield; j) piperidine/CH_2Cl_2 / r.t. / 4 h / 89%; TFA/H_2O /37 °C / 4 h/ 76%; k) $CuSO_4 \cdot H_2O$ / sodium ascorbate / MeOH/CH_2Cl_2 / r.t. / 14 h / 93%; l) piperidine/CH_2Cl_2 / r.t. / 4 h / 84%; TFA/H_2O /r.t. / 4 h / 52%.

Methylated cellobiose derivatives **2a** and **3a** were prepared in order to optimize reaction conditions for the methylcellulose derivatives. Copper-assisted azide-alkyne cycloaddition (CuAAC, the "click reaction") of 2,3,4,6-tetra-*O*-methyl-β-D-glucopyranosyl-(1→4)-2,3,6-tri-*O*-methyl-β-D-glucopyranosyl azide (**7a**) and propargylated peptide segments **9** and **10** afforded methylated cellobiose derivatives **5a** (85% yield) and **6a** (87% yield) bearing peptide residues, respectively. Subsequent deprotections of the peptide segments gave methylated cellobioses **2a** and **3a** end-functionalized with peptides.

The optimized reaction conditions for the cellobiose derivatives allowed us to synthesize the peptide-functionalized methylcelluloses **2b** and **3b**. The CuAAC reactions of tri-*O*-methylcellulosyl azide (**7b**) and propargylated peptide segments **9** and **10** afforded methylcelluloses **5b** and **6b** end-functionalized with protected peptides, respectively; deprotection of the peptide segments of these compounds afforded peptide-functionalized methylcelluloses **2b** and **3b**.

While tri-*O*-methylcellulosyl azide (**7b**) is a mixture of both α- and β-anomers, the cellobiosyl azide **7a** is only the β-anomer. Moreover, each methylcellulose derivative **7b**, **4b**, **5b**, **6b**, **1b**, **2b**, and **3b** bears a single hydroxyl group at the C-4 position of its methylated glucosyl residue furthest from the azide. In contrast, cellobiosyl azide derivative **7a** has no such hydroxyl group. We have reported the synthesis of blockwise alkylated (1→4) linked trisaccharides, and found that the anomeric configuration between the hydrophobic and hydrophilic segments affects surface activity of the aqueous solution (Nakagawa et al. 2011c).

Characterization

Figure 1 displays the ^{1}H-NMR spectra of cellobiose derivatives **1a**, **2a**, and **3a** acquired in deuterium oxide. Proton resonances are assigned on the basis of two-dimensional NMR experiments (see experimental section). The triazole protons of compounds **1a**, **2a**, and **3a** appear at 8.24, 8.19, and 8.24 ppm, respectively. Carbon resonances of compounds **1a**, **2a**, and **3a** have also been assigned (see experimental section). Interestingly, the triazole proton of compound **3a** appears as a broad singlet. The methylene protons of compound **3a** adjacent to the triazole ring also appear as a broad peak at about 4.40–4.61 ppm. In addition, the C-1 proton of the cellobiosyl residue appears as a broad doublet at 5.75 ppm.

The transverse relaxation times T_2s of triazole proton and C1 proton adjacent to the triazole of anionic compound **3a** would be shorter than that of compounds **1a** and **2a**, although molecular weights of compounds **1a**, **2a**, and **3a** are similar. The transverse relaxation times T_2s of protons of an anionic surfactant, sodium dodecyl sulfate (SDS), depend on their positions; T_2s of the internal protons are shorter than that of methyl protons and methylene protons adjacent to the sulfate group (Yu et al. 2017). The transverse relaxation time T_2s of the protons of anionic compound **3a** showed the same tendency as the anionic surfactant, SDS.

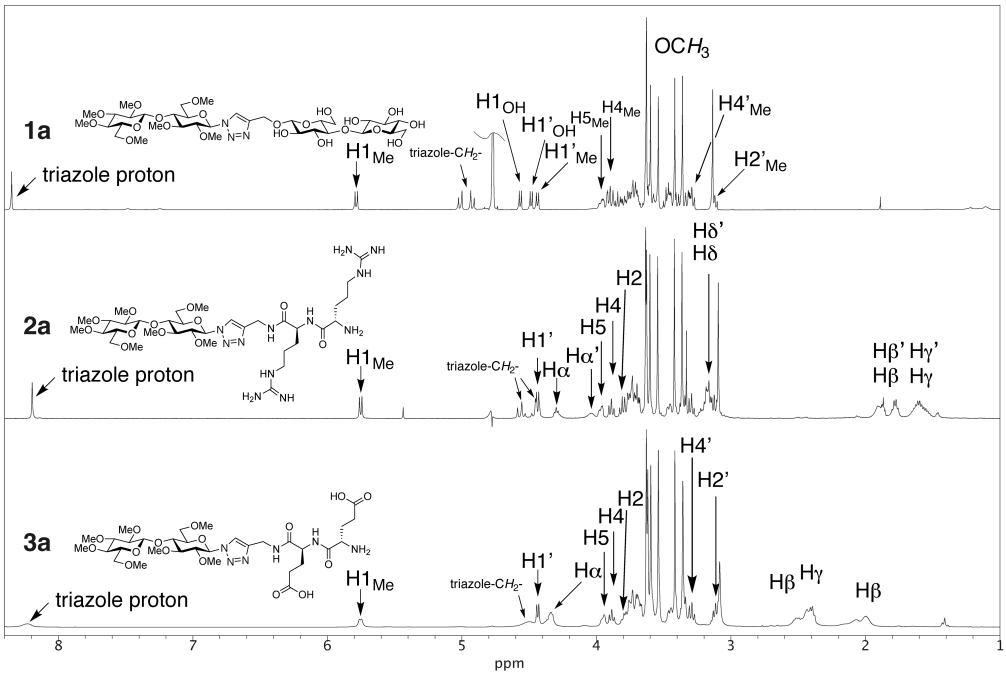

232

233 **Figure 1.** 500-MHz ^{1}H-NMR spectra of compounds **1a**, **2a**, and **3a** in D_2O.

234

235 Figure 2 displays the MALDI-TOF MS spectra of compounds **1a**, **2a**, and **3a**.
236 Pseudomolecular sodium $[M+Na]^+$ and potassium $[M+K]^+$ adduct-ion peaks
237 corresponding to compound **1a** appear at *m*/*z* 868.6 and 884.6, respectively. The
238 pseudomolecular proton adduct-ion peak $[M+H]^+$ of compound **2a** appears at *m*/*z*
239 833.6, while pseudomolecular proton $[M+H]^+$, sodium $[M+Na]^+$, and potassium
240 $[M+K]^+$ adduct-ion peaks of compound **3a** appear at *m*/*z* 779.5, 801.5, and 817.5,
241 respectively.

242

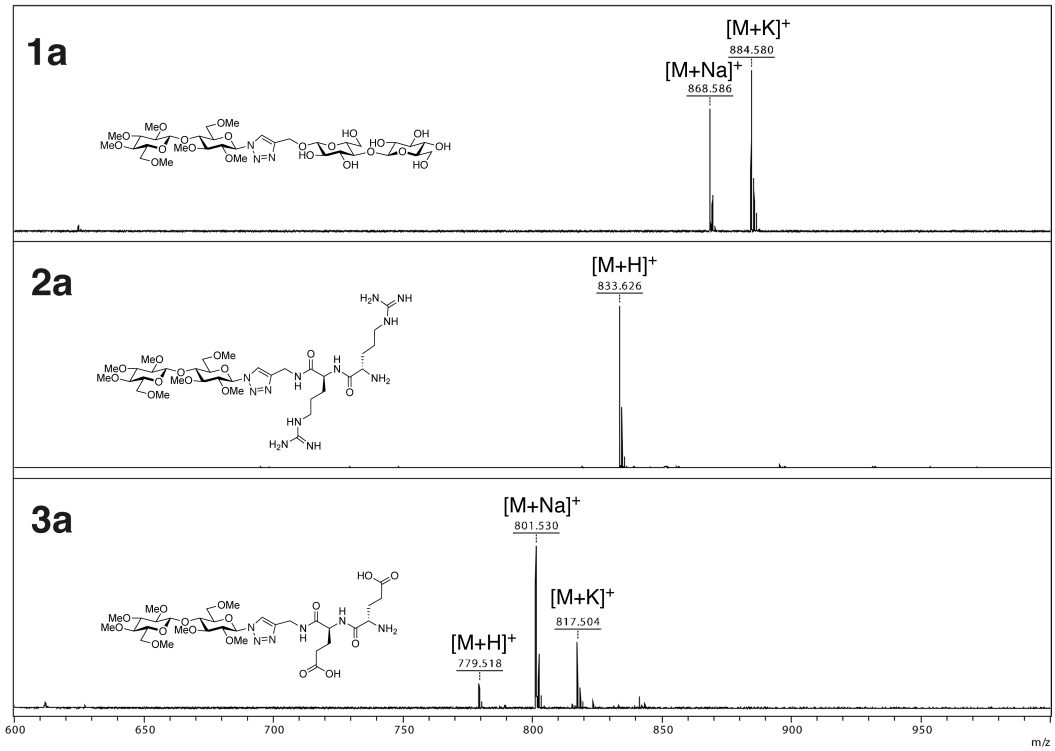

Figure 2. MALDI-TOF MS spectra of compounds **1a**, **2a**, and **3a**.

In summary, the NMR and MALDI-TOF MS data for cellobiose derivatives **1a**, **2a**, and **3a** reveal that the conditions for the CuAAC reactions and the deprotections of the peptide residues are appropriate. Hence, the reaction conditions developed for these cellobiose derivatives were used to synthesize the peptide-functionalized methylcelluloses **1b**, **2b**, and **3b**.

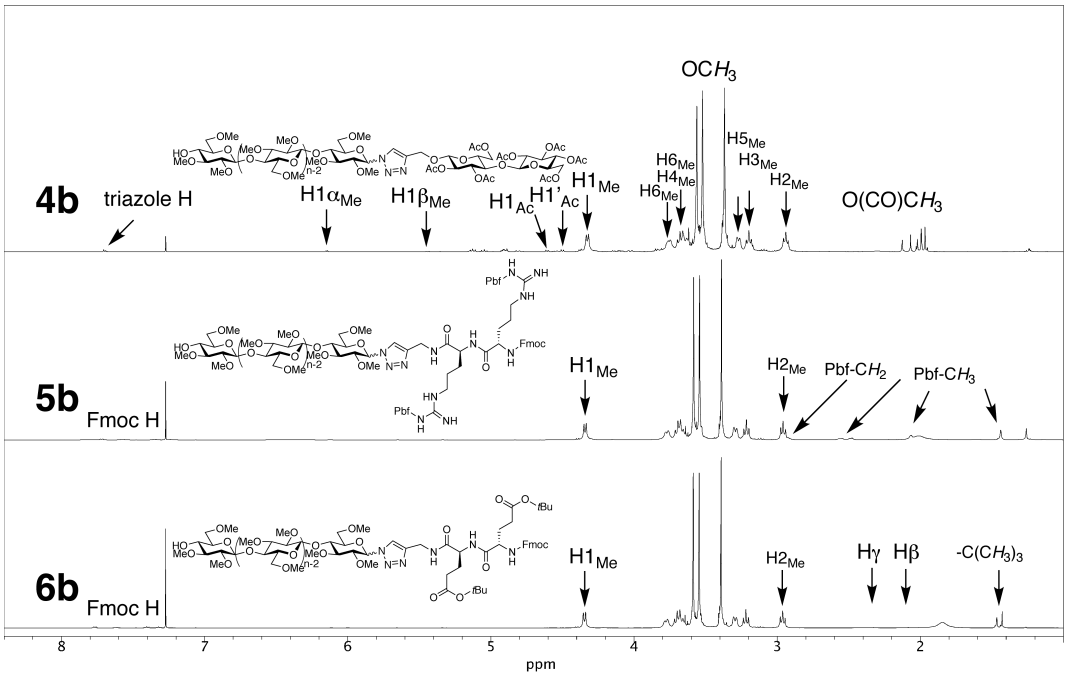

Figure 3. ^{1}H-NMR spectra of compounds **4b**, **5b**, and **6b** in $CDCl_3$.

Compounds **5b** and **6b** as well as the trehalose-type diblock methylcellulose analogue **4b** (Yamagami et al. 2018), as an authentic sample of a methylcellulose end-functionalized with a peptide, were synthesized according to the optimized reaction conditions for cellobiose derivatives **5a** and **6a**, as well as **4a**. Figure 3 displays the ^{1}H-NMR spectra of compounds **4b**, **5b**, and **6b** acquired in $CDCl_3$. The triazole proton of compound **4b** appears at 7.69 (β-anomer) and 7.70 (α-anomer) ppm (α/β ratio = 2/1) (Yamagami et al. 2018), while the triazole protons of compounds **5b** and **6b** were unable to be identified due to overlapping resonances associated with the aromatic protons of their Fmoc groups, although proton resonances of the peptide side-chains were observed.

The same deprotection procedures used for the cellobiosyl compounds **1a**, **2a**, and **3a** were used for the polymeric compounds, to give methylcellulose derivatives **1b**, **2b**, and **3b**. Figure 4 displays the ^{1}H-NMR spectra of

methylcellulose derivatives **1b**, **2b**, and **3b** acquired in D_2O. Resonances corresponding to the peptide moieties at the methylcellulose ends are not clearly evident in their spectra because of the higher DP of the methylcellulose residues, compared to the cellobiosyl compounds **1a**, **2a**, and **3a**, as shown in Figure 1. However, the triazole protons of compounds **2b** and **3b** appear at 8.42 and 8.43 ppm, respectively, although those of compound **1a** appear at 8.42, 8.35, and 8.27 ppm. This fact indicates that compounds **2b** and **3b** are end-functionalized with peptide residues. The zeta potential of compounds **1b**, **2b**, and **3b** summarized in Table 1 also indicate that the deprotections of compounds **2b** and **3b** were successful.

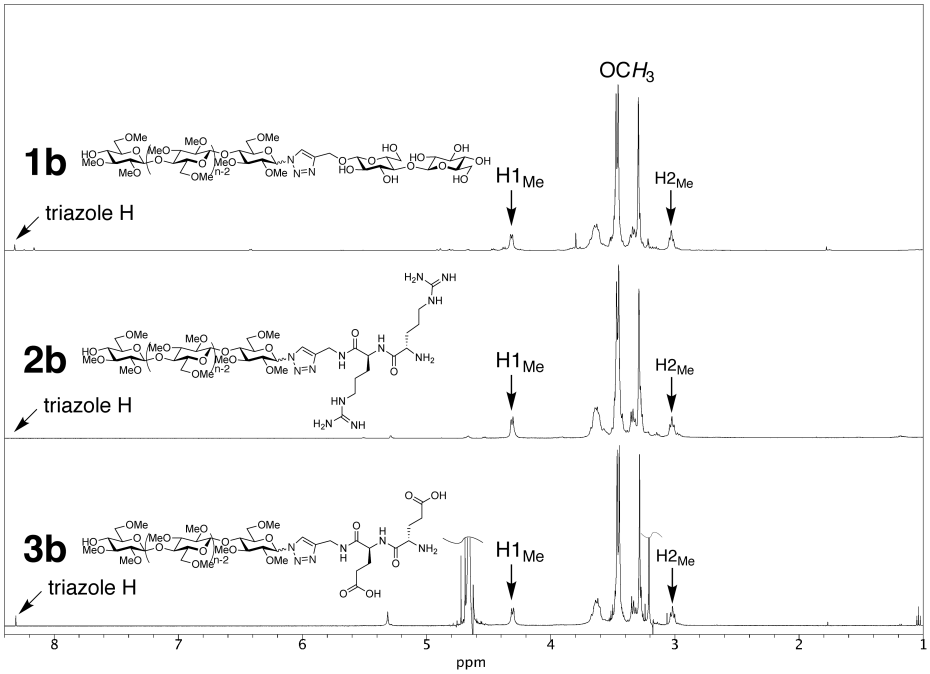

Figure 4. ^{1}H-NMR spectra of compounds **1b**, **2b**, and **3b** in D_2O.

Figure 5 displays the FT-IR spectra of compounds **2b**, **3b**, **5b**, **6b**, **7b**, **9**, and **10**. Infrared absorption peaks corresponding to the protected di(arginine) and di(glutamic acid) segments **9** and **10** appear in the spectra of methylcelluloses **5b**

and **6b** end-functionalized with the di(arginine), and di(glutamic acid) derivatives, respectively. The infrared absorption peak associated with methylcellulosyl azide **7b** was observed at 2116 cm^{-1}. After the Huisgen 1,3-dipolar cycloaddition of **7b** with the di(arginine) or di(glutamic acid) derivatives **9** or **10**, infrared absorption peaks associated with the azido group were not evident in the spectra of **5b** and **6b**, which indicates that the Huisgen 1,3-dipolar cycloadditions were successful. The infrared spectra of compounds **5b** and **6b** changed during deprotection to give **2b** and **3b**. The infrared absorption peaks corresponding to Pbf and Fmoc groups of MC-*b*-(Arg(Pbf))$_2$-Fmoc **5b** were not evident in the spectrum of MC-*b*-ArgArg **2b**. The infrared absorption peaks associated with the *t*Bu and Fmoc groups of MC-*b*-(Glu(O*t*Bu))$_2$-Fmoc **6b** were not evident in the spectrum of MC-*b*-GluGlu **3b**. The FT-IR analyses of the end-functionalized methylcellulose derivatives provide us with additional experimental data regarding the polymer reactions that occur at the ends of these macromolecules. We conclude that methylcelluloses **2b** and **3b** end-functionalized with peptides were successfully synthesized.

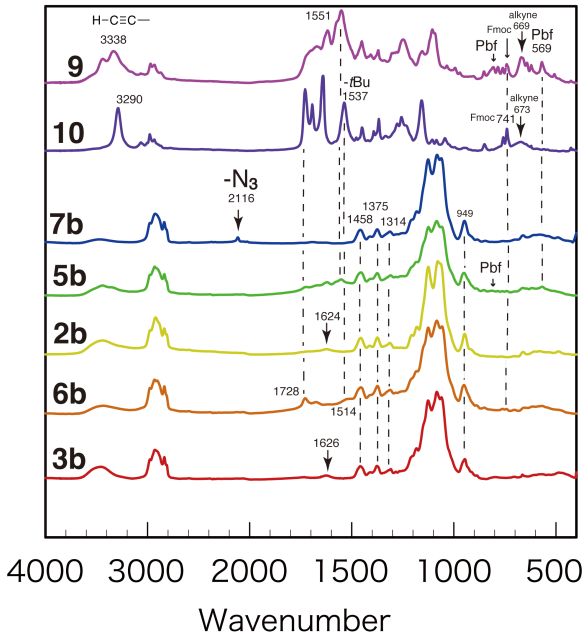

Figure 5. FT-IR spectra of compounds **2b**, **3b**, **5b**, **6b**, **7b**, **9**, and **10**.

Physical properties of compounds 1b, 2b, and 3b

Table 1 summarizes the structures, solution surface tensions, and zeta potentials of compounds **1b**, **2b**, and **3b**, while Figure 6 shows the surface tensions of solutions of compounds **1b**, **2b**, and **3b** as functions of concentration, measured at 23 °C. Compounds **2b** and **3b** exhibited similar surface-tension curves; the critical micelle concentrations (CMCs) of the arginine-containing compound **2b** and the glutamic-acid-containing compound **3b** are both 0.0035 mg/mL, slightly lower than that of the cellobiose derivative **1b** (0.008 mg/mL). An ionic peptide residue at the end of the methylcellulose unit improves its surface activity compared to that of methylcellulose end-functionalized with the nonionic cellobiosyl residue. In contrast, the CMCs of methylcelluloses **2b** and **3b** end-functionalized with peptides (0.0035 mg/mL) are clearly lower than that of commercial SM-4 methylcellulose (0.1 mg/mL).

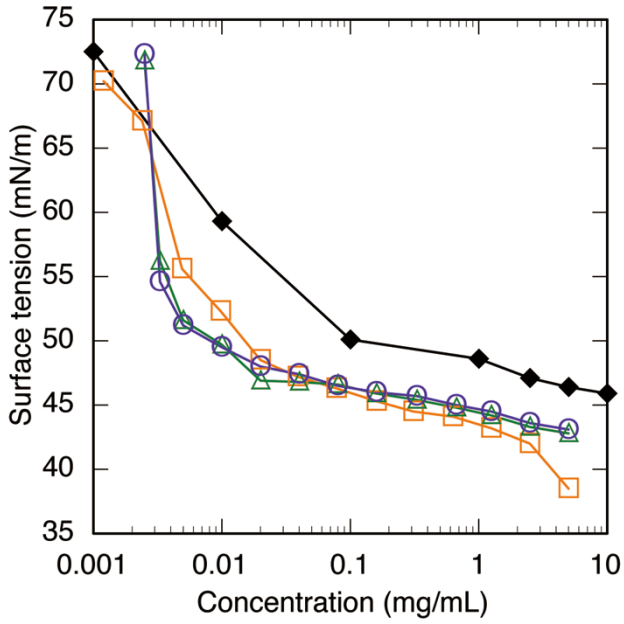

Figure 6. Surface tensions of compounds **1b**, (orange open squares), **2b** (green open triangles), and **3b** (purple open circles), and commercial MC (black solid diamonds), as functions of concentration.

317

318 **Table 1**. Surface tensions and zeta potentials of compounds **1b**, **2b**, and **3b**.

Comp. No.	Hydrophilic segment	DP_n of hydrophobic segment	DS	Surface tension (mN/m) at CMC	Critical micelle concentration (mg/mL)	Zeta potential (mV)
MC			1.8	50.1	0.1	
1b	Cellobiose	20.7	2.65	49.0	0.008	−11.5
2b	Arginine dimer	27.3	–	47.3	0.0035	−7.5
3b	Glutamic acid dimer	32.8	–	49.3	0.0035	−14.1

319

320 Figure 7 displays the temperature-dependence of the supramolecular
321 aggregation behavior of compounds **1b**, **2b**, and **3b** in water, obtained by dynamic
322 light scattering (DLS) experiments. The hydrodynamic diameters of compounds
323 **1b**, **2b**, and **3b** at 25 °C were determined to be 138, 706, and 476 nm, respectively.
324 Although the hydrodynamic diameter of commercial MC SM-4 gradually
325 increased at temperatures above approximately 45 °C, those of compounds **1b**, **2b**,
326 and **3b** increased dramatically at 33 °C, 30 °C, and 31 °C, respectively.

327

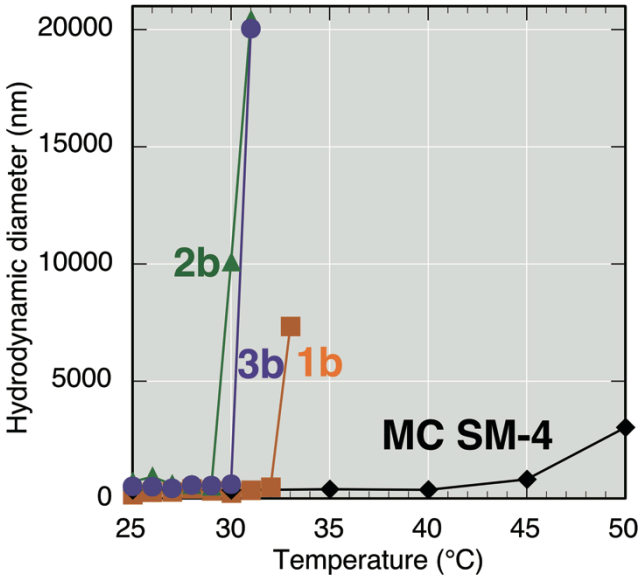

Figure 7. Hydrodynamic diameters of 0.2 wt% aqueous solutions of compounds **1b** (orange solid squares), **2b** (green solid triangles), **3b** (purple solid circles), and commercial MC (black solid diamonds) as functions of temperature.

Figure 8 shows the DSC thermograms of 2 wt% aqueous solutions of compounds **2b** and **3b**. Endothermic peaks appear at 31.5 °C and 32.6 °C for compounds **2b** and **3b**, respectively. The endothermic temperatures of compounds **2b** and **3b** are closely related to the supramolecular aggregation temperatures determined by DLS. The endothermic peaks observed by DSC are attributed to dehydration around the peptide-end-functionalized MCs **2b** and **3b**. Dehydration around these cellulosic molecules promotes their supramolecular aggregation, as shown in Figure 7.

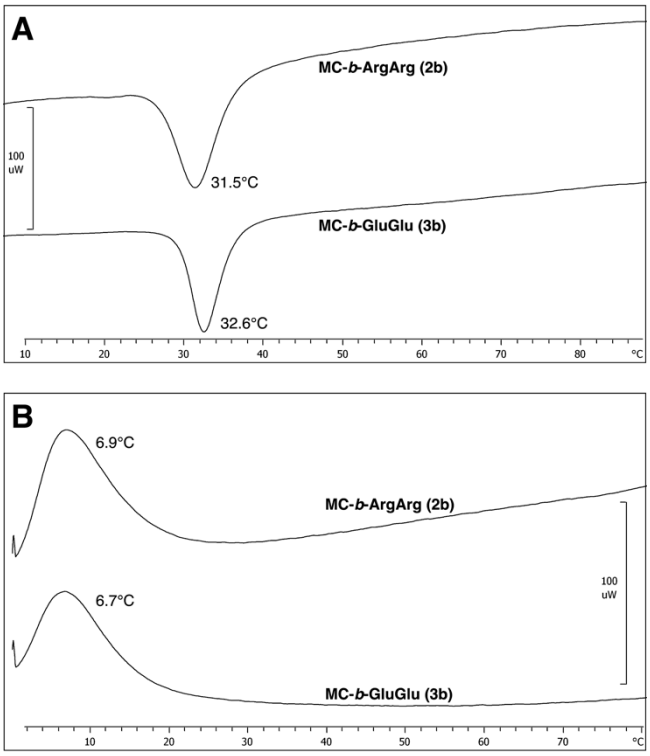

341 **Figure 8.** DSC thermograms of 2.0 wt% aqueous solutions of compounds **2b** and **3b**: (A) heating
342 curves (3.5 °C/min) and (B) cooling curves (3.5 °C/min).

343

344 Table 2 displays images of 2.0 and 4.0 wt% aqueous solutions of compounds **1b**,
345 **2b**, and **3b** at 0 and 35 °C. The 2 wt% aqueous solution of the cellobiose-
346 functionalized MC **1b** forms a hydrogel at 35 °C. In contrast, the peptide-
347 functionalized MCs **2b** and **3b** do not form hydrogels at 35 °C, rather their
348 solutions became turbid at this temperature. In other words, the 2.0 wt% aqueous
349 solutions of **2b** and **3b** phase separate at 35 °C. However, 4.0 wt% aqueous
350 solutions of **1b**, **2b**, and **3b** form hydrogels at 35 °C. The concentrations of the
351 thermally induced supramolecular structures of **2b** and **3b** are the keys to forming
352 thermo-reversible hydrogels because 4.0 wt% aqueous solutions of the peptide-
353 functionalized MCs **2b** and **3b** form hydrogels at 35 °C.

354

355

356 **Table 2.** Images of 2.0 and 4.0 wt% aqueous solutions of compounds **1b**, **2b**, and **3b**.

Comp. No.	Concentration: 2.0 wt %		Concentration: 4.0 wt %	
	Temperature (°C)		Temperature (°C)	
	0	35	0	35
1b				
2b				
3b				

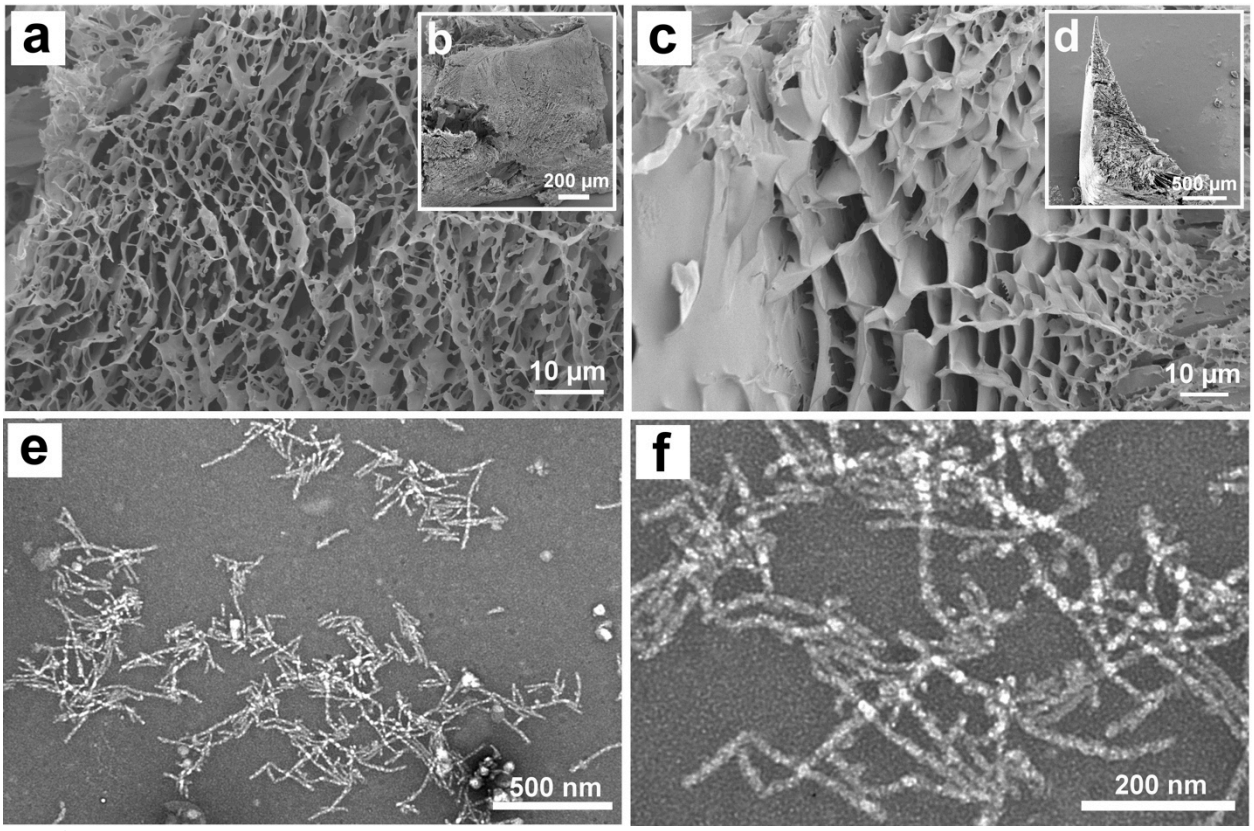

357

358 **Figure 9.** SEM images of the hydrogels of (a, b) **2b** and (c, d) **3b**. (e, f) TEM images of the
359 hydrogel of **2b**. Insets (b) and (d) are enlargements of regions in panels (a) and (c).

360

Lyophilized hydrogels from compounds 2b and 3b

SEM images of lyophilized hydrogels of **2b** and **3b** are shown in Figures 9a–d. We previously reported that methylcellulose end-functionalized with cellobiose exhibits a layered structure (Yamagami et al. 2018). In contrast, the peptide-functionalized methylcelluloses **2b** and **3b** form a three-dimensional mesh structure (**2b**) and a spongy, foam-like structure (**3b**), indicating that the hydrophilic segments at the ends of the methylcellulose units of the lyophilized hydrogels have different nanostructures.

TEM images of the nanostructure of the thermoresponsive supramolecular hydrogel of 2b

TEM images of the hydrogel of compound **2b** are shown in Figures 9e–f, in which regular stick-like structures with orthogonal widths of approximately 12 nm and 15 nm, can be seen. The widths of the stick-like structures are constant, although their lengths vary widely. The molecular length of compound **2b** is ~16 nm, which suggests that the longer width of a single rectangular structure is likely to correspond to the molecular length of compound **2b**. The average thickness of these structures was determined by atomic force microscopy to be approximately 10 nm (data not shown). Rectangular self-assemblies appear to form stick-like structures, and their entanglements produce a macroscopic hydrogel.

Drug release from thermoresponsive supramolecular hydrogel matrices

The thermo-reversible supramolecular hydrogels of MCs **2b** and **3b** end-functionalized with cationic and anionic peptides, respectively, are expected to interact with anionic and cationic compounds, respectively. Therefore, we investigated the ionic drug-release behavior of these hydrogels. To that end,

386 diclofenac sodium and imipramine were selected as model anionic and cationic
387 drugs, respectively.

388 Figure 10 displays the drug-release behavior of the thermoresponsive
389 supramolecular hydrogel matrices of **1b**, **2b**, and **3b**. These matrices exhibit
390 almost the same release behavior for diclofenac sodium (DFNa) at 37 °C at the
391 start of release testing. Approximately 28–29% of the DFNa was released from
392 hydrogel matrices **1b**, **2b**, and **3b** after 1 h. After 12 h, ~81% of the DFNa was
393 released from cationic hydrogel matrix **2b**, while ~100% of the DFNa was
394 released from the nonionic and anionic hydrogel matrices **1b** and **3b**. This
395 observation indicates that the cationic di(arginine) segment at the end of the MC
396 affects the release behavior of the anionic DFNa from the thermoresponsive
397 supramolecular hydrogel matrix.

398 In contrast, cationic imipramine interacts with anionic supramolecular hydrogel
399 matrix **3b**. At the beginning of imipramine-release testing (after 1 h of incubation)
400 27%, 28%, and 22% of the imipramine was released from hydrogel matrices **1b**,
401 **2b**, and **3b**, respectively. After 12 h, 98%, 96%, and 81% of the imipramine was
402 released from hydrogel matrices **1b**, **2b**, and **3b**, respectively, which indicates that
403 the anionic di(glutamic acid) segment at the end of the MC interacts with the
404 cationic imipramine. Ionic interactions between the cationic imipramine and the
405 anionic hydrogel matrix **3b** promote the relatively slow release of imipramine
406 from the thermoresponsive supramolecular hydrogel matrix.

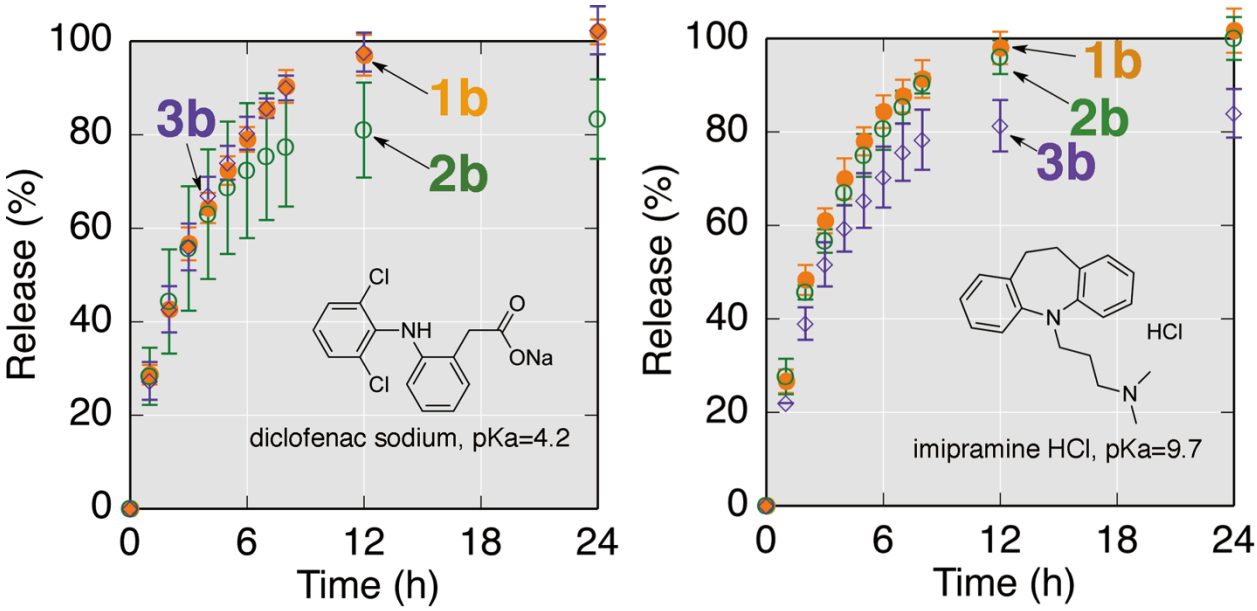

407

408 **Figure 10.** Drug-release behavior from the thermoresponsive supramolecular hydrogel matrices of
409 **1b** (orange solid circles), **2b** (green open circles), and **3b** (purple open diamonds).

410

411 To gain deep insight into the interaction between the model drugs and the MCs
412 end-functionalized with peptides, we performed ^{1}H-NMR experiments involving
413 DFNa, methylated cellobiose derivative **2a** (a model compound of the MC end-
414 functionalized with di(arginine) **2b**), and a mixture of DFNa and **2a**, in deuterium
415 oxide.

416 Figure 11 reveals changes in the chemical shifts corresponding to both
417 compounds, namely DFNa and **2a**, following mixing. After mixing anionic DFNa
418 and cationic **2a** in D_2O, the proton resonances of DFNa, numbered 1 to 8, were
419 observed to shift downfield by 0.007, 0.010, 0.020, 0.033, 0.019, 0.019, 0.019,
420 and 0.009 ppm, respectively, which indicates that all of the protons in DFNa
421 became deshielded through the removal of electron density. In contrast, the
422 methylene protons of the arginine side-chain appear at higher magnetic fields
423 following mixing, which indicate that these protons have became shielded due to
424 an increase in electron density. In addition, the triazole proton of **2a**, which

425 resonated at 8.19 ppm prior to mixing, also appeared at slightly higher magnetic
426 field following mixing with DFNa.
427 These observations indicate that supramolecular hydrogels of methylcellulose
428 end-functionalized with ionic peptides are expected to not only be
429 thermoresponsive but also pH responsive. This temperature/pH dual-
430 responsivenesses of compounds **2b** and **3b** are currently under investigation.
431

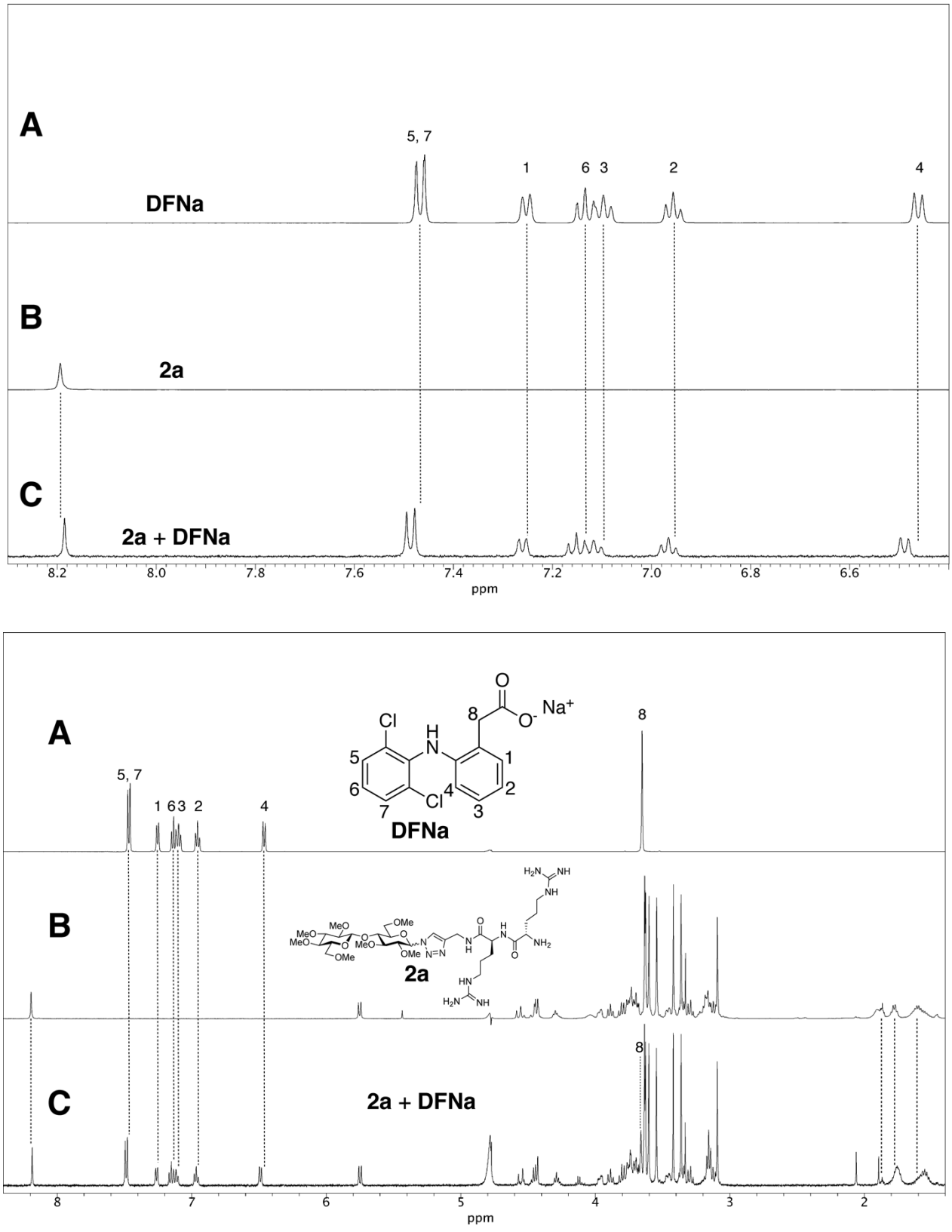

Figure 11. ^{1}H-NMR analyses of the interactions between compound **2b** and diclofenac sodium.

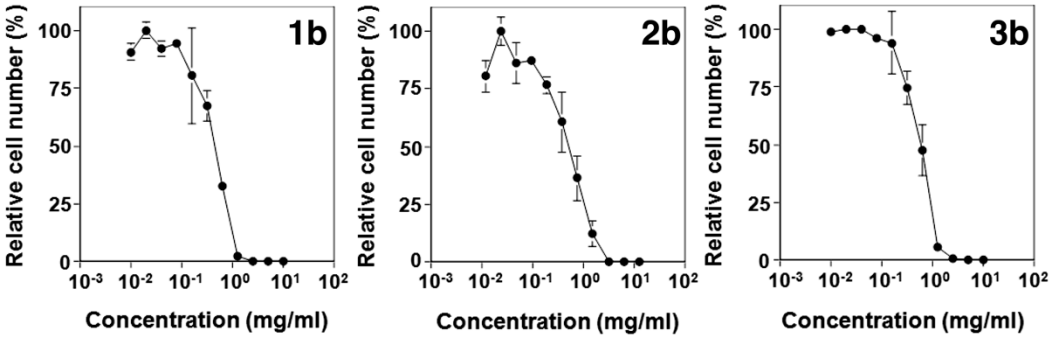

Figure 12. Inhibition of U937 cell growth by compounds **1b**, **2b**, and **3b**.

Cytotoxicities of compounds 1b, 2b, and 3b

ATP-based U937 histocytoma cell-viability assays reveal that the half maximal inhibitory concentrations (IC_{50} values) of compounds **1b**, **2b**, and **3b** were 470, 560, and 600 μg/mL, respectively, as shown in Figure 12. As previously noted, 4 wt% aqueous solutions (40 mg/mL) of compounds **2b** and **2c** become supramolecular thermoresponsive hydrogels at 37 °C (see Table 2). The hydrogelation of an aqueous solution of compound **2b** or **2c** is likely to inhibit cell growth of suspension-type cells such as U937. However, the cytotoxicities of aqueous solutions of compounds **2b** and **2c**, determined by IC_{50} values, have been evaluated correctly, despite some supramolecular structures potentially present in the aqueous solutions. In summary, methylcelluloses end-functionalized with peptides are essentially nontoxic to U937 histocytoma cells because IC_{50} values of 0.6 wt% are considerably high.

Conclusion

Aqueous solutions of methylcelluloses end-functionalized with peptides exhibit supramolecular thermoresponsive hydrogelation behavior equivalent to those of block-functionalization methylcelluloses (Nakagawa et al. 2011a; Nakagawa et al. 2012c; Yamagami et al. 2018). The tri-*O*-methylcellulose block, as a hydrophobic segment (Kamitakahara et al. 2016), is a key structure for supramolecular

thermoresponsive hydrogelation. Investigation into the relationships between the anomeric configuration at the reducing-end of the tri-*O*-methylcellulose block and physico-chemical properties in solution is now in progress. We were able to not only introduce carbohydrates (Yamagami et al. 2018) but also peptides as hydrophilic segments at the ends of hydrophobic tri-*O*-methylcellulose units, resulting in the syntheses of a pool of diblock methylcellulose analogues with biological functions that retain thermoresponsive hydrogelation behavior at human-body temperature. As methylcellulose is produced from cellulose, which is a natural resource, methylcelluloses end-functionalized with peptides are expected to be used in biomedical applications as, for example, comparatively safe injectable hydrogels.

Experimental Section

Materials.

*N*α-(9-Fluorenylmethoxycarbonyl)-*N*ω-(2,2,4,6,7-pentamethyldihydrobenzofuran-5-sulfonyl)-L-arginine (*N*α-Fmoc-*N*ω-Pbf-L-arginine) was purchased from Watanabe Chemical Industries, Ltd., Japan. *N*α-(9-Fluorenylmethoxycarbonyl)glutamic acid γ-tert-butyl ester monohydrate (Fmoc-Glu(O*t*-Bu)-OH) was purchased from Peptide Institute, Inc., Japan. Other chemicals were purchased from Nacalai Tesque, Wako Pure Chemicals, Tokyo Chemical Industry, and Sigma-Aldrich. All reagents and solvents were of commercial grade and were used without further purification.

Synthesis.

_N_α-Fmoc-_N_ω-Pbf-L-arginine-_N_-propargylamide (12)

*N*α-Fmoc-*N*ω-Pbf-L-arginine-*N*-propargylamide (**12**) (Yang et al. 2011) was prepared from *N*α-Fmoc-*N*ω-Pbf-L-arginine (**11**) (89% yield). Briefly, to a solution of *N*α-Fmoc-*N*ω-Pbf-L-arginine (**11**, 200 mg) in methanol (5 mL) was added propargylamine (19 μL) and 4-(4,6-dimethoxy-1,3,5-triazin-2-yl)-4-methylmorpholinium chloride (DMT-MM, 102 mg). The reaction mixture was stirred for 3 h under nitrogen. The crude product was purified by preparative silica-gel thin-layer chromatography (PTLC, eluent: 10% MeOH/CH_2Cl_2) to give compound **12** (188 mg, 89% yield).

^{1}H-NMR (500 MHz, $CDCl_3$): δ 1.42 (6H, CH_3, Pbf), 1.55-1.58 (m, 2H, Hγ), 1.85 (m, 2H, Hβ), 2.07 (s, 3H, CH_3, Pbf), 2.14 (t, 1H, *J*=2.0 Hz, $CH_2CC\underline{H}$), 2.50 (s, 3H, CH_3, Pbf), 2.57 (s, 3H, CH_3, Pbf), 2.91 (s, 2H, CH_2, Pbf), 3.28 (m, 2H, Hδ), 3.98 (m, 2H, $C\underline{H_2}CCH$), 4.14 (t, 1H, *J*=7.0 Hz, CH, Fmoc), 4.27 (m, 1H, Hα), 4.34 (d, 2H, *J*=7.0 Hz, Fmoc), 7.24-7.74 (arom. Fmoc)

^{13}C-NMR (125 MHz, $CDCl_3$): δ 12.4 (CH_3, Pbf), 17.9 (CH_3, Pbf), 19.3 (CH_3, Pbf), 25.2 (Cγ), 28.5 (CH_3, Pbf), 29.1 ($\underline{C}H_2CCH$), 30.1 (Cβ), 40.5 (Cδ), 43.1 ($\underline{C}H_2$, Pbf), 46.9 ($\underline{C}H$, Fmoc), 54.1 (Cα), 67.1 ($\underline{C}H_2$, Fmoc), 71.3 ($CH_2C\underline{C}H$), 79.4 ($CH_2\underline{C}CH$), 86.4 (C, Pbf), 117.5 (arom. Pbf), 119.9 (arom. Fmoc), 124.7 (arom. Pbf), 125.1 (arom. Fmoc), 127.0 (arom. Fmoc), 127.7 (arom. Fmoc), 132.3 (arom. Pbf), 138.4 (arom. Pbf), 141.1 (arom. Fmoc), 143.6 (arom. Fmoc), 143.7 (arom. Fmoc), 156.3, 156.6 (CO Fmoc, quaternary C of guanidino group of arginine), 158.9 (-O-$\underline{C}$ arom. Pbf), 172.1 (Arg, Cα-$\underline{C}$O-NH-)

***N*ω-Pbf-L-arginine-*N*-propargylamide (13)**

*N*α-Fmoc-*N*ω-Pbf-L-arginine-*N*-propargylamide (**12**, 200 mg) was dissolved in 50% piperidine/dichloromethane (2 mL). The reaction mixture was stirred for 1 h at room temperature under nitrogen, after which it was concentrated to dryness.

The crude product was extracted with ethyl acetate, washed with water and brine, dried over sodium sulfate, and concentrated to dryness. The residue was purified by silica-gel column chromatography (eluent: 15% methanol/dichloromethane, v/v) to afford compound **13** (111 mg, 82% yield).

^{1}H-NMR (500 MHz, $CDCl_3$): δ 1.47 (6H, CH_3, Pbf), 1.56-1.63 (m, 2H, Hγ), 1.80 (m, 2H, Hβ), 2.09 (s, 3H, CH_3, Pbf), 2.22 (t, 1H, *J*=2.0 Hz, $CH_2CC\underline{H}$), 2.50 (s, 3H, CH_3, Pbf), 2.57 (s, 3H, CH_3, Pbf), 2.96 (s, 2H, CH_2, Pbf), 3.22 (m, 2H, Hδ), 3.45 (t, 1H, Hα), 3.98 (m, 2H, $C\underline{H_2}CCH$),

^{13}C-NMR (125 MHz, $CDCl_3$): δ 12.4 (CH_3, Pbf), 17.9 (CH_3, Pbf), 19.3 (CH_3, Pbf), 25.4 (Cγ), 28.5 (CH_3, Pbf), 28.8 ($\underline{C}H_2CCH$), 31.9 (Cβ), 40.6 (Cδ), 43.2 ($\underline{C}H_2$, Pbf), 54.2 (Cα), 71.3 ($CH_2C\underline{C}H$), 79.6 ($CH_2\underline{C}CH$), 86.4 (C, Pbf), 117.5 (arom. Pbf), 124.6 (arom. Pbf), 132.2 (arom. Pbf), 138.2 (arom. Pbf), 156.4 (quaternary C of guanidino group of arginine), 158.9 (-O-$\underline{C}$ arom. Pbf), 175.1 (Arg, Cα-$\underline{C}$O-NH-)

***N*α-Fmoc-*N*ω-Pbf-L-arginine-*N*ω-Pbf-L-arginine-*N*-propargylamide** (**9**) (Morelli and Matile 2017)

To a solution of *N*α-Fmoc-*N*ω-Pbf-L-arginine (**11**, 101 mg, 1.2 equiv.) and *N*ω-Pbf-L-arginine-*N*-propargylamide (**13**, 60 mg, 1.0 equiv.) in methanol (5 mL) was added DMT-MM (43 mg, 1.2 equiv.). The reaction mixture was stirred for 4 h at room temperature under nitrogen, and then concentrated to dryness. The crude product was purified by PTLC (eluent: 10% methanol/dichloromethane) to afford compound **9** as colorless crystals (126 mg, 89% yield).

^{1}H-NMR (500 MHz, $CDCl_3$): δ 1.42 (12H, CH_3, Pbf), 1.63 (m, 4H, Hγ), 1.78 (m, 2H, Hβ), 1.92 (m, 2H, Hβ), 2.05 (s, 3H, CH_3, Pbf), 2.06 (s, 3H, CH_3, Pbf), 2.09 (1H, $CH_2CC\underline{H}$), 2.48 (s, 3H, CH_3, Pbf), 2.49 (s, 3H, CH_3, Pbf), 2.55 (s, 3H,

530 CH_3, Pbf), 2.57 (s, 3H, CH_3, Pbf), 2.90 (s, 2H, CH_2, Pbf), 2.91 (s, 2H, CH_2, Pbf),
531 3.21 (m, 4H, Hδ), 3.91-3.96 (m, 2H, $C\underline{H_2}CCH$), 4.09 (t, 1H, *J*=7.0 Hz, CH, Fmoc),
532 4.27 (broad t, 1H, Hα), 4.32-4.36 (d, d, 1H, 1H, *J*=7.0 Hz, Fmoc), 7.17-7.73
533 (arom. Fmoc)
534 ^{13}C-NMR (125 MHz, $CDCl_3$): δ 12.4 (CH_3, Pbf), 17.9 (CH_3, Pbf), 19.3 (CH_3,
535 Pbf), 25.6 (Cγ), 28.5 (CH_3, Pbf), 29.1 ($\underline{C}H_2CCH$), 29.1 (Cβ), 40.0 (Cδ), 40.6 (Cδ),
536 43.1 ($\underline{C}H_2$, Pbf), 46.9 ($\underline{C}$H, Fmoc), 53.5 (Cα), 55.1 (Cα), 67.3 ($\underline{C}H_2$, Fmoc), 71.3
537 ($CH_2C\underline{C}H$), 79.4 ($CH_2\underline{C}CH$), 86.4 (CH, Fmoc), 117.6 (arom. Pbf), 119.9 (arom.
538 Fmoc), 124.7 (arom. Pbf), 125.1 (arom. Fmoc), 127.0 (arom. Fmoc), 127.7 (arom.
539 Fmoc), 132.3 (arom. Pbf), 138.4 (arom. Pbf), 141.1 (arom. Fmoc), 143.7 (arom.
540 Fmoc), 156.4, 157.0 (CO Fmoc, quaternary C of guanidino group of arginine),
541 158.9 (-O-$\underline{C}$ arom. Pbf), 172.0 (Arg, Cα-$\underline{C}$O-NH-), 173.4 (Arg, Cα-$\underline{C}$O-NH-)
542 MALDI-TOF MS (*m/z*): calcd for $C_{56}H_{73}N_9O_{10}S_2$, 1095.49; found, $[M+Na]^+$ =
543 1116.2

544 FT-IR (KBr): 3440, 3338, 2970, 2934, 1670, 1618, 1551, 1450, 1369, 1248, 1155,
545 1105, 853, 806, 783, 760, 741 (Fmoc), 669, 642, 621, 569 (Pbf, -SO_2NH-) cm^{-1}

546

547 **Fmoc-Glu(O*t*-Bu)-*N*-propargylamide** (**15**) (Aagren et al. 2006)
548 To a solution of Fmoc-Glu(O*t*-Bu)-OH (**14**, 300 mg) in methanol (5 mL) was
549 added propargylamine (52 μL) and DMT-MM (102 mg). The reaction mixture
550 was stirred for 3 h under nitrogen. The crude product was purified by PTLC
551 (eluent: 10% MeOH/CH_2Cl_2) to give compound **15** as colorless crystals (324 mg,
552 quantitative yield).

553 ^{1}H-NMR (500 MHz, $CDCl_3$): δ 1.47 (s, 9H, CH_3, *t*Bu), 1.96 (m, 1H, Hβ), 2.09
554 (m, 1H, Hβ), 2.22 (t, 1H, *J*=2.0 Hz, CH_2CCH), 2.33 (m, 1H, Hγ), 2.43 (m, 1H,
555 Hγ), 4.05 (broad s, 2H, CH_2CCH), 4.21 (2H, CH Fmoc, Hα), 4.41 (m, 2H, Fmoc),
556 5.78 (d, 1H, *J*=7.5 Hz, NH), 6.70 (broad s, 1H, NH), 7.32 (dt, 2H, *J*=1.0 Hz, *J*=7.5
557 Hz, Fmoc), 7.32 (dt, 2H, *J*=1.0 Hz, *J*=1.0 Hz, Fmoc), 7.41 (dt, 2H, *J*=1.0 Hz,
558 Fmoc), 7.77 (d, 2H, *J*=7.5 Hz, Fmoc),

559 ^{13}C-NMR (125 MHz, $CDCl_3$): δ 28.0 (CH_2CCH), 28.0 (CH_3, *t*Bu), 39.2 (Cβ),
560 31.6 (Cγ), 47.1 (CH, Fmoc), 54.1 (Cα), 67.1 (CH_2, Fmoc), 71.8 (CH_2CCH), 79.1
561 (CH_2CCH), 81.2 (quaternary C of *t*Bu), 120.0 (arom. Fmoc), 125.0 (arom. Fmoc),
562 127.1 (arom. Fmoc), 127.7 (arom. Fmoc), 141.3 (arom. Fmoc), 143.7 (arom.
563 Fmoc), 156.3 (CO Fmoc), 171.0 (Glu, -Cα-CO-NH-), 173.0 (Glu, CδOO *t*Bu)

564 MALDI-TOF MS (*m/z*): calcd for $C_{27}H_{30}N_2O_5$, 462.22; found, $[M+Na]^+$ = 485.2,
565 $[M+K]^+$ = 501.2

566

567 **Glu(O*t*-Bu)-*N*-propargylamide** (**16**) (Aagren et al. 2006)

568 Fmoc-Glu(O*t*-Bu)-*N*-propargylamide (**15**, 308 mg) was dissolved in 50%
569 piperidine/dichloromethane (2 mL). The reaction mixture was stirred for 1 h at
570 room temperature under nitrogen, after which it was concentrated to dryness. The
571 crude product was extracted with ethyl acetate, washed with water and brine,
572 dried over sodium sulfate, and concentrated to dryness. The residue was purified
573 by silica-gel column chromatography (eluent: dichloromethane; eluent: 5%
574 methanol/dichloromethane, v/v) to afford compound **16** (166 mg, quantitative
575 yield).

576 ^{1}H-NMR (500 MHz, $CDCl_3$): δ 1.45 (s, 9H, CH_3 (*t*Bu)), 1.83 (m, 1H, Hβ), 2.09
577 (m, 1H, Hβ), 2.23 (t, 1H, *J*=2.0 Hz, CH_2CCH), 2.35 (m, 2H, Hγ), 3.44 (t, 1H, Hα),
578 4.05 (broad s, 2H, CH_2CCH),

579 ^{13}C-NMR (125 MHz, $CDCl_3$): δ 28.0 (CH_3 (tBu)), 28.8 ($\underline{C}H_2CCH$), 30.1 (Cβ),
580 31.9 (Cγ), 54.4 (Cα), 71.4 ($CH_2C\underline{C}H$), 79.6 ($CH_2\underline{C}CH$), 80.7 ($\underline{C}(CH_3)_3$), 172.8
581 (Glu, -Cα-$\underline{C}$O-NH-), 174.1 (Glu, $\underline{C}$δOO *t*Bu)
582 MALDI-TOF MS (*m/z*): calcd for $C_{12}H_{20}N_2O_3$, 240.15; found, $[M+Na]^+$ = 263.9
583
584 ***N*α-Fmoc-Glu(O*t*-Bu)-Glu(O*t*-Bu)-*N*-propargylamide (10)**
585 To a solution of Fmoc-Glu(O*t*-Bu)-OH (**14**, 328 mg, 1.2 equiv.) and Glu(O*t*-
586 Bu)-*N*-propargylamide (**16**, 148 mg, 1.0 equiv.) in methanol (5 mL) was added
587 DMT-MM (204 mg, 1.2 equiv.). The reaction mixture was stirred for 1 h at room
588 temperature under nitrogen, and then concentrated to dryness. The crude product
589 was purified by PTLC (eluent: 5% methanol/dichloromethane) to afford
590 compound **10** as colorless crystals (378 mg, 95% yield).
591 ^{1}H-NMR (500 MHz, $CDCl_3$): δ 1.43 (s, 9H, CH_3 (*t*Bu)), 1.47 (s, 9H, CH_3 (*t*Bu)),
592 1.96-2.15 (m, 4H, Hβ), 2.13 ((t, 1H, *J*=2.0 Hz, $CH_2CC\underline{H}$), 2.33-2.47 (m, 4H, Hγ),
593 3.96-4.03 (broad s, 2H, $C\underline{H_2}CCH$), 4.20 (1H, H (Fmoc)), 4.20-4.24 (1H, Hα),
594 4.38-4.44 (m, 2H, CH_2 (Fmoc)), 4.48-4.49 (m, 1H, Hα), 7.30-7.77 (8H, arom.
595 Fmoc)
596 ^{13}C-NMR (125 MHz, $CDCl_3$): δ 27.0 (Cβ'), 27.4 (Cβ), 28.0 (CH_3 (tBu)), 29.1
597 ($\underline{C}H_2CCH$), 30.1 31.7 (Cγ'), 31.8 (Cγ), 52.6 (Cα'), 55.2 (Cα), 67.3 (CH_2, Fmoc),
598 71.3 ($CH_2C\underline{C}H$), 79.4 ($CH_2\underline{C}CH$), 81.1 ($\underline{C}(CH_3)_3$), 81.3 ($\underline{C}(CH_3)_3$), 120.0, 125.1,
599 127.0, 127.7, 141.2, 143.7, 156.5, 170.6 (Glu, -Cα-$\underline{C}$O-NH-), 171.6 (Glu, -Cα-
600 $\underline{C}$O-NH-), 173.0 (Glu, $\underline{C}$δOO *t*Bu), 173.2 (Glu, $\underline{C}$δOO *t*Bu)
601 MALDI-TOF MS (*m/z*): calcd for $C_{36}H_{45}N_3O_8$, 647.32; found, $[M+Na]^+$ = 670.4
602 FT-IR (KBr): 3290, 2978, 1728, 1694, 1639, 1537 (*t*Bu), 1450, 1368, 1258,
603 1157, 851, 758, 741 (Fmoc), 673 cm^{-1}

2,3,4,6-Tetra-*O*-methyl-β-D-glucopyranosyl-(1→4)-2,3,6-tri-*O*-methyl-β-D-glucopyranosyl azide (7a)

A 60% suspension of sodium hydride in mineral oil (1.97 g, 82.1 mmol, 14.0 equiv.) was added to a solution of β-D-glucopyranosyl-(1→4)-β-D-glucopyranosyl azide (Schamann and Schafer 2003; Ying and Gervay-Hague 2003) (1.29 g, 3.51 mmol) in DMF (30 mL) at 0 °C. The mixture was stirred at 0 °C for 1 h under nitrogen. Methyl iodide (3.1 mL, 49.8 mmol, 14.2 equiv.) was then added to the reaction mixture at 0 °C. After 2 h, the mixture was warmed to room temperature and stirred for 2 h. The reaction was monitored by analytical thin-layer chromatography (TLC). Methanol (0.43 mL) was added to deactivate the sodium hydride. The mixture was concentrated and the crude product was extracted with ethyl acetate, washed with distilled water, brine, dried over Na_2SO_4, and concentrated to dryness. The residue was purified by silica-gel column chromatography (eluent: 2:1 (v/v) ethyl acetate/*n*-hexane) to give colorless crystals (**7a**, 0.799 g, 49% yield).

^{1}H-NMR (500 MHz, $CDCl_3$): δ 2.86 (dd, 1H, *J*=8.0 Hz, *J*=8.5 Hz, H2'), 1H, 2.90 (t, 1H, *J*=9.0 Hz, H3'), 3.06 (t, 1H, *J*=9.5 Hz, H3'), 3.12 (t, 1H, *J*=9.5 Hz, H4'), 3.16 (ddd, 1H, *J*=2.0 Hz, *J*=4.0 Hz, *J*=9.5 Hz, H5'), 3.19 (t, 1H, *J*=9.0 Hz, H3), 3.32 (s, 3H, OCH_3), 3.34 (s, 3H, OCH_3), 3.36 (ddd, 1H, *J*=2.0 Hz, *J*=4.0 Hz, *J*=10.0 Hz, H5), 3.46 (s, 3H, OCH_3), 3.48 (s, 3H, OCH_3), 3.52 (dd, 1H, *J*=4.0 Hz, *J*=11.0 Hz, H6), 3.53 (s, 6H, OCH_3), 3.56 (s, 3H, OCH_3), 3.56 (dd, 1H, *J*=2.0 Hz, *J*=10.5 Hz, H6'), 3.62 (dd, 1H, *J*=9.0 Hz, *J*=10.0 Hz, H4), 3.63 (dd, 1H, *J*=2.0 Hz, *J*=11.0 Hz, H6), 3.67 (dd, 1H, *J*=4.0 Hz, *J*=11.0 Hz, H6), 4.23 (d, 1H, *J*=7.5 Hz, H1'), 4.40 (d, 1H, *J*=8.5 Hz, H1)

^{13}C-NMR (125 MHz, $CDCl_3$): δ 103.2 (C1'), 89.9 (C1), 86.9 (C3'), 84.9 (C3), 84.0 (C2'), 82.8 (C2), 79.3 (C4'), 77.2 (C4), 76.9 (C5), 74.7 (C5'), 71.2 (C6'), 70.1 (C6), 60.8, 60.6, 60.6, 60.6, 60.3, 59.3, 59.2 (O*C*H$_3$)

Tri-*O*-methylcellulosyl azide (**7b**) Compound **7b** was prepared according to our previous paper (Kamitakahara et al. 2016).

FT-IR (KBr): 3478, 2926, 2836, 2116 (N_3), 1458, 1375, 1314, 1182, 1061, 949, 664 cm^{-1}

2-Propynyl 2,3,6-tri-*O*-acetyl-β-D-glucopyranosyl-(1→4)-2,3,6-tri-*O*-acetyl-β-D-glucopyranoside (8) Compound **8** was prepared according to our previous paper (Yamagami et al. 2018).

1-[2,3,4,6-Tetra-*O*-methyl-β-D-glucopyranosyl-(1→4)-2,3,6-tri-*O*-methyl-β-D-glucopyranosyl]-4-[2,3,4,6-tetra-*O*-acetyl-β-D-glucopyranosyl-(1→4)-2,3,6-tri-*O*-acetyl-β-D-glucopyranosyloxymethyl]-1*H*-1,2,3-triazole (4a)

Azide **7a** (117 mg, 0.252 mmol) and glycoside **8** (170 mg, 0.252 mmol) were dissolved in DMF (9 mL). Copper(I) bromide (361.5 mg, 2.52 mmol, 10 equiv.), sodium ascorbate in water (998.5 mg/1.26 mL, 20 equiv.), and *N*,*N*,*N*′,*N*″,*N*″-pentamethyldiethylenetriamine (PMDETA, MW = 173.3, *d* = 0.83 g/mL, 0.5 mL, 10 equiv.) were added to the solution at room temperature. The reaction mixture was stirred for 21 h. The insoluble component was then removed by filtration and washed with dichloromethane. The washings and filtrate were combined and concentrated, and the DMF was azeotropically removed with ethanol. The crude product was purified by silica-gel column chromatography (eluent: 10%

MeOH/CH_2Cl_2) to give 1-[2,3,4,6-tetra-*O*-methyl-β-D-glucopyranosyl-(1→4)-2,3,6-tri-*O*-methyl-β-D-glucopyranosyl]-4-[2,3,4,6-tetra-*O*-acetyl-β-D-glucopyranosyl-(1→4)-2,3,6-tri-*O*-acetyl-β-D-glucopyranosyloxymethyl]-1*H*-1,2,3-triazole (**4a**, 161.3 mg, 56% yield).

^{1}H-NMR (500 MHz, $CDCl_3$): δ 1.97, 1.99, 2.01, 2.01, 2.04, 2.09, 2.15 (CO*C*H_3), 2.95 (t, 1H, *J*=8.5 Hz, H2'$_{Me}$), 3.15 (t, 1H, *J*=9.0 Hz, H3'$_{Me}$), 3.19 (s, 3H, OCH_3), 3.21 (t, 1H, *J*=9.0 Hz, H4'$_{Me}$), 3.26 (ddd, 1H, *J*=2 Hz, *J*=3.5 Hz, *J*=9.5 Hz, H5'$_{Me}$), 3.33 (s, 3H, OCH_3), 3.43 (s, 3H, OCH_3), 3.44 (t, 1H, *J*=9.0 Hz, H3$_{Me}$), 3.55 (s, 3H, OCH_3), 3.57 (s, 3H, OCH_3), 3.64 (s, 6H, OCH_3), 3.6-3.7 (H6'$_{Me}$, H2$_{Me}$, H5$_{Me}$, H5$_{Ac}$, H5'$_{Ac}$), 3.75 (dd, 1H, *J*=4.0 Hz, *J*=11.0 Hz, H6$_{Me}$), 3.79 (t, 1H, *J*=9.5 Hz, H4$_{Ac}$), 3.82 (dd, 1H, *J*=9.0 Hz, *J*=10.0 Hz, H4$_{Me}$), 4.05 (dd, 1H, *J*=2.5 Hz, *J*=12.5 Hz, H6$_{Ac}$), 4.11 (dd, 1H, *J*=5.0 Hz, *J*=12.0 Hz, H6'$_{Ac}$), 4.34 (d, 1H, *J*=8.0 Hz, H1'$_{Me}$), 4.36 (dd, 1H, *J*=4.0 Hz, *J*=12.0 Hz, H6$_{Ac}$), 4.52 (d, 1H, *J*=8.0 Hz, H1'$_{Ac}$), 4.56 (dd, 1H, *J*=2.0 Hz, *J*=12.0 Hz, H6'$_{Ac}$), 4.62 (d, 1H, *J*=8.0 Hz, H1$_{Ac}$), 4.81 (d, 1H, *J*=13.0 Hz, OC*H*$_2$-triazole), 4.92 (d, 1H, *J*=13.0 Hz, OC*H*$_2$-triazole), 4.9-4.95 (H2$_{Ac}$, H2'$_{Ac}$), 5.07 (t, 1H, *J*=9.5 Hz, H4'$_{Ac}$), 5.15 (t, 1H, *J*=9.0 Hz, H3$_{Ac}$) , 5.15 (t, 1H, *J*=9.0 Hz, H3'$_{Ac}$), 5.47 (d, 1H, *J*=9.5 Hz, H1$_{Me}$), 7.69 (s, 1H, triazole)

^{13}C-NMR (125 MHz, $CDCl_3$): δ 20.5, 20.6, 20.6, 20.9 (CO*C*H_3), 59.0 (O*C*H_3), 59.4 (O*C*H_3), 60.3 (O*C*H_3), 60.4 (O*C*H_3), 60.7 (O*C*H_3), 60.7 (O*C*H_3), 60.8 (O*C*H_3), 61.5(C6'$_{Ac}$), 61.7 (C6$_{Ac}$), 62.8 (OC*H*$_2$-triazole), 67.8 (C4'$_{Ac}$), 70.0 (C6$_{Me}$), 71.2 (C6'$_{Me}$), 71.4 (C2$_{Ac}$ or C2'$_{Ac}$), 71.6 (C2$_{Ac}$ or C2'$_{Ac}$), 72.0 (C5$_{Ac}$), 72.4 (C5'$_{Ac}$), 72.8 (C3$_{Ac}$ or C3'$_{Ac}$), 72.9 (C3$_{Ac}$ or C3'$_{Ac}$), 74.8 (C5'$_{Me}$), 76.3(C4$_{Ac}$), 77.9 (C4$_{Me}$), 79.3 (C4'$_{Me}$), 82.1 (C2$_{Me}$), 84.0 (C2'$_{Me}$), 85.2 (C3$_{Me}$), 87.0 (C3'$_{Me}$), 87.3 (C1$_{Me}$), 99.6 (C1$_{Ac}$), 100.7 (C1'$_{Ac}$), 103.3 (C1'$_{Me}$), 122.0 (triazole *C*H), 144.3 (O-CH_2-*C*=), 169.0, 169.3, 169.6, 169.7, 170.2, 170.5 (CO*C*H_3)

1-[2,3,4,6-Tetra-*O*-methyl-β-D-glucopyranosyl-(1→4)-2,3,6-tri-*O*-methyl-β-D-glucopyranosyl]-4-[β-D-glucopyranosyl-(1→4)-β-D-glucopyranosyloxymethyl]-1*H*-1,2,3-triazole (1a)

Sodium methoxide (28%) in methanol (0.01 mL, 1.4 equiv.) was added at room temperature to a solution of 1-[2,3,4,6-tetra-*O*-methyl-β-D-glucopyranosyl-(1→4)-2,3,6-tri-*O*-methyl-β-D-glucopyranosyl]-4-[2,3,4,6-tetra-*O*-acetyl-β-D-glucopyranosyl-(1→4)-2,3,6-tri-*O*-acetyl-β-D-glucopyranosyloxymethyl]-1*H*-1,2,3-triazole (**4a**, 146 mg, 0.128 mmol) in MeOH (1 mL) and THF (1 mL). The mixture was stirred for 3 h at room temperature. The solution was neutralized with Amberlyst H^+. The Amberlyst H^+ was removed by filtration and washed with MeOH. The combined filtrate and washings were concentrated to dryness to give 1-[2,3,4,6-tetra-*O*-methyl-β-D-glucopyranosyl-(1→4)-2,3,6-tri-*O*-methyl-β-D-glucopyranosyl]-4-[β-D-glucopyranosyl-(1→4)-β-D-glucopyranosyloxymethyl]-1*H*-1,2,3-triazole (**1a**, 108.3 mg, quantitative yield).

^{1}H-NMR (500 MHz, D_2O): δ 3.01 (t, 1H, *J*=9.5 Hz, $H2'_{Me}$), 3.03 (s, 3H, OCH_3), 3.18 (t, 1H, *J*=10.0 Hz, $H4'_{Me}$), 3.21 ($H2_{OH}$), 3.21 ($H2'_{OH}$), 3.25 (t, 1H, *J*=10.0 Hz, $H3'_{Me}$), 3.25 (s, 3H, OCH_3), 3.28 ($H4'_{OH}$), 3.31 (s, 3H, OCH_3), 3.33-3.38 (m, 1H, $H5_{OH}$), 3.36 (t, 1H, *J*=9.0 Hz, $H3'_{OH}$), 3.38 ($H5'_{Me}$), 3.43 (s, 3H, OCH_3), 3.49 (s, 3H, OCH_3), 3.5 ($H3_{OH}$), 3.50-3.56 ($H4_{OH}$), 3.52 (s, 6H, OCH_3), 3.56-3.7 ($H6_{Me}$ and $H6'_{Me}$), 3.58-3.86 ($H6_{OH}$ and $H6'_{OH}$), 3.62 ($H3_{Me}$), 3.73 (t, 1H, *J*=9.0 Hz, $H2_{Me}$), 3.79 (t, 1H, *J*=10.0 Hz, $H4_{Me}$), 3.86 (m, 1H, $H5_{Me}$), 4.33 (d, 1H, *J*=8.0 Hz, $H1'_{Me}$), 4.38 (d, 1H, *J*=8.5 Hz, $H1'_{OH}$), 4.46 (d, 1H, *J*=7.5 Hz, $H1_{OH}$), 4.81 (d, 1H, *J*=13.0 Hz, OC$\underline{H}_2$-triazole), 4.90 (d, 1H, *J*=13.0 Hz, OC$\underline{H}_2$-triazole), 5.68 (d, 1H, *J*=9.0 Hz, $H1_{Me}$), 8.24 (s, 1H, triazole C*H*)

703 ^{13}C-NMR (125 MHz, D_2O): δ 61.0 (O<u>C</u>H_3), 61.1 (O<u>C</u>H_3), 62.3 (O<u>C</u>H_3), 62.6
704 (O<u>C</u>H_3), 62.6 ($C6_{OH}$ or $C6'_{OH}$), 62.7 (O<u>C</u>H_3), 63.2 (O<u>C</u>H_3), 63.2 ($C6_{OH}$ or $C6'_{OH}$),
705 64.6 (OC<u>H_2</u>-triazole), 72.1 ($C4'_{OH}$), 72.4 ($C6_{Me}$ or $C6'_{Me}$), 73.1 ($C6_{Me}$ or $C6'_{Me}$),
706 75.4 ($C2'_{OH}$), 75.8 ($C2_{OH}$), 76.1 ($C3'_{OH}$), 76.9 ($C3_{OH}$), 77.4 ($C5_{OH}$), 78.1 ($C5_{OH}$ or
707 $C5'_{Me}$), 78.6 ($C4_{Me}$), 78.7 ($C5_{OH}$ or $C5'_{Me}$), 79.3 ($C5_{Me}$), 81.1 ($C4_{OH}$), 81.4 ($C4'_{Me}$),
708 83.9 ($C2_{Me}$), 85.4 ($C2'_{Me}$), 86.0 ($C3_{Me}$), 87.6 ($C3'_{Me}$), 88.9 ($C1_{Me}$), 104.1 ($C1_{OH}$),
709 105.1 ($C1'_{Me}$), 105.2 ($C1'_{OH}$), 127.5 (triazole *C*H), 146.9 (O-CH_2-*C*=)
710 MALDI-TOF MS (*m/z*): calcd for $C_{34}H_{59}N_3O_{21}$, 845.36; found, $[M+Na]^+$ =
711 868.586, $[M+K]^+$ = 884.580
712
713 **1-(2,3,6-Tri-*O*-methyl-cellulosyl)-4-[2,3,4,6-tetra-*O*-acetyl-β-D-**
714 **glucopyranosyl-(1→4)-2,3,6-tri-*O*-acetyl-β-D-glucopyranosyloxymethyl]-1*H*-**
715 **1,2,3-triazole** (**4b**)
716 Compound **4b** was prepared according to our previous paper (Yamagami et al.
717 2018). GPC analysis: $M_n = 7.4 \times 10^3$, $M_w / M_n = 1.4$, $DP_n = 34.8$.
718
719 **1-(2,3,6-Tri-*O*-methyl-cellulosyl)-4-[β-D-glucopyranosyl-(1→4)-β-D-**
720 **glucopyranosyloxymethyl]-1*H*-1,2,3-triazole** (**1b**)
721 Compound **1b** was prepared according to our previous paper (Yamagami et al.
722 2018). GPC analysis: $M_n = 6.8 \times 10^3$, $M_w / M_n = 1.4$, $DP_n = 33$.
723
724 **1-[2,3,4,6-Tetra-*O*-methyl-β-D-glucopyranosyl-(1→4)-2,3,6-tri-*O*-methyl-β-**
725 **D-glucopyranosyl]-4-(*N*α-Fmoc-*N*ω-Pbf-L-arginine-*N*ω-Pbf-L-arginine-*N*-**
726 **methyl)-1*H*-1,2,3-triazole** (**5a**)

To a solution of 2,3,4,6-tetra-*O*-methyl-β-D-glucopyranosyl-(1→4)-2,3,6-tri-*O*-methyl-β-D-glucopyranosyl azide (**7a**, 25 mg, 0.054 mmol) and Fmoc-Arg(Pbf)-Arg(Pbf)-NH-CH_2CCH (**9**, 59 mg, 0.054 mmol) in 3 mL of methanol/dichloromethane (1/4, v/v) were added CuBr (77 mg, 0.054 mmol, 10 equiv.) and aqueous sodium ascorbate (213 mg/269 μL). The reaction mixture was stirred under nitrogen at room temperature for 2 h. The mixture was purified by preparative TLC (eluent: 1:9 (v/v) methanol/dichloromethane) to give 1-[2,3,4,6-tetra-*O*-methyl-β-D-glucopyranosyl-(1→4)-2,3,6-tri-*O*-methyl-β-D-glucopyranosyl]-4-(*N*α-Fmoc-*N*ω-Pbf-L-arginine-*N*ω-Pbf-L-arginine-*N*-methyl)-1*H*-1,2,3-triazole (**5a**, 71 mg, 0.045 mmol, 85% yield).

^{1}H-NMR (500 MHz, $CDCl_3$): δ: 1.44 (C*H*$_3$, Pbf), 1.59 (Hγ), 1.85 (Hβ), 2.06-2.09 (CH_3, Pbf), 2.49-2.59 (CH_3, Pbf), 2.92 (CH_2, Pbf), 2.94 (CH_2, Pbf), 2.92 (t, 1H, *J*=9.0 Hz, H2'$_{Me}$), 3.11 (OC*H*$_3$), (3.12 (t, 1H, *J*=9.0 Hz, H3'$_{Me}$), 3.15 (t, 1H, *J*=9.0 Hz, H4'$_{Me}$), 3.21-3.25 (m, 1H, H5'$_{Me}$), 3.22 (OC*H*$_3$), 3.26 (Hδ), 3.40 (OC*H*$_3$), 3.35 (t, 1H, *J*=8.5 Hz, H3$_{Me}$), 3.38 (OC*H*$_3$), 3.52 (OC*H*$_3$), 3.53 (OC*H*$_3$), 3.59 (OC*H*$_3$), 3.62 (OC*H*$_3$), 3.5-3.7 (H6'$_{Me}$, H2$_{Me}$, H5$_{Me}$), 3.6-3.75 (2H, H6$_{Me}$), 3.75 (t, 1H, *J*=9.5 Hz, H4$_{Me}$), 4.1-4.35 (broad s, Hα), 4.18-4.24 (1H, H (Fmoc)), 4.30 (H1'$_{Me}$), 4.32-4.36 (C*H*$_2$, Fmoc), 4.43-4.60 (broad d, broad d, 2H, NH-C*H*$_2$-triazole), 5.41 (H1$_{Me}$), 5.60 (NH), 6.0-6.6 (NH), 7.2-7.8 (arom. H, Fmoc)

^{13}C-NMR (125 MHz, $CDCl_3$): δ 12.5 (CH_3, Pbf), 17.9 (CH_3, Pbf), 19.3 (CH_3, Pbf), 25.6 (Cγ), 28.6 (CH_3, Pbf), 29.7 (Cβ), 40.8 (Cδ), 43.2 (CH_2, Pbf), 47.0 (CH, Fmoc), 53.6 (Cα), 54.4 (Cα), 58.7, 59.3, 60.4, 60.6, 60.8 (O*C*H$_3$), 67.3 (CH_2, Fmoc), 70.1 (C6), 71.2 (C6'), 74.7 (C5'), 77.2 (C4), 77.4 (C5), 79.3 (C4'), 81.8 (C2), 84.0 (C2'), 85.2 (C3), 86.4 (CH, Fmoc), 86.4 (CH, Fmoc), 86.9 (C3'), 87.0 (C1), 103.3 (C1'), 117.6 (arom. Pbf), 119.9 (arom. Fmoc), 120.0, 122.5 (triazole

752 *C*H), 124.6 (arom. Pbf), 124.9 (arom. Fmoc), 125.2 (arom. Fmoc), 127.1 (arom.
753 Fmoc), 127.6 (arom. Fmoc), 132.3 (arom. Pbf), 132.7 (arom. Pbf), 138.3 (arom.
754 Pbf), 141.1 (arom. Fmoc), 143.7 (arom. Fmoc), 144.5 (O-CH_2-*C*=), 156.4 (arom.
755 Pbf), 158.7 (-O-C arom. Pbf), 172.2 (Arg, Cα-CO-NH-), 173.5 (Arg, Cα-CO-NH)
756 MALDI-TOF MS (*m/z*): calcd for $C_{75}H_{108}N_{12}O_{20}S_2$, 1560.72; found, $[M+H]^+$ =
757 1559.755, $[M+Na]^+$ = 1581.722, $[M+K]^+$ = 1597.671
758
759 **1-[2,3,4,6-Tetra-*O*-methyl-β-D-glucopyranosyl-(1→4)-2,3,6-tri-*O*-methyl-β-**
760 **D-glucopyranosyl]-4-(Arg-Arg-NH-CH_2)-1*H*-1,2,3-triazole (2a)**
761 1-[2,3,4,6-Tetra-*O*-methyl-β-D-glucopyranosyl-(1→4)-2,3,6-tri-*O*-methyl-β-D-
762 glucopyranosyl]-4-(*N*α-Fmoc-*N*ω-Pbf-L-arginine-*N*ω-Pbf-L-arginine-*N*-methyl)-
763 1*H*-1,2,3-triazole (**5a**, 61 mg, 0.039 mmol) was dissolved in
764 piperidine/dichloromethane (1/1, v/v, 1 mL). The reaction mixture was stirred
765 under nitrogen at room temperature for 1 h and then concentrated to dryness. The
766 crude product was purified by preparative TLC (eluent: 15:85 (v/v)
767 methanol/dichloromethane) to give 1-[2,3,4,6-tetra-*O*-methyl-β-D-
768 glucopyranosyl-(1→4)-2,3,6-tri-*O*-methyl-β-D-glucopyranosyl]-4-(*N*ω-Pbf-L-
769 arginine-*N*ω-Pbf-L-arginine-*N*-methyl)-1*H*-1,2,3-triazole (34 mg, 0.025 mmol,
770 65% yield; MALDI-TOF MS (*m/z*): calcd for $C_{60}H_{96}N_{12}O_{18}S_2$, 1336.64; found,
771 $[M+Na]^+$ = 1359.5).
772 1-[2,3,4,6-Tetra-*O*-methyl-β-D-glucopyranosyl-(1→4)-2,3,6-tri-*O*-methyl-β-D-
773 glucopyranosyl]-4-(*N*ω-Pbf-L-arginine-*N*ω-Pbf-L-arginine-*N*-methyl)-1*H*-1,2,3-
774 triazole (31 mg, 0.023 mmol) was dissolved in TFA/distilled water (8/2, v/v, 1.0
775 mL) and stirred under nitrogen at 37 °C for 4 h. The reaction mixture was
776 concentrated to dryness and the crude product was purified by gel-filtration

column chromatography (LH-20, eluent: methanol) to give 1-[2,3,4,6-tetra-*O*-methyl-β-D-glucopyranosyl-(1→4)-2,3,6-tri-*O*-methyl-β-D-glucopyranosyl]-4-(Arg-Arg-NH-CH_2)-1*H*-1,2,3-triazole (**2a**, 10 mg, 0.012 mmol, 52% yield).

^{1}H-NMR (500 MHz, D_2O): δ 1.5-1.7 (m, 4H, Hγ and Hγ'), 1.73-1.83 (m, 2H, Hβ), 1.85-1.95 (m, 2H, Hβ'), 3.09 (s, 3H, OCH_3), 3.12 (t, *J*=9.5 Hz, H2'), 3.12-3.25 (m, 4H, Hδ and Hδ'), 3.29 (t, *J*=9.0 Hz, H4'), 3.36 (t, *J*=9.0 Hz, H3'), 1H, 3.36 (s, 3H, OCH_3), 3.42 (s, 3H, OCH_3), 3.46 (m, 1H, H5'), 3.54 (s, 3H, OCH_3), 3.60 (s, 3H, OCH_3), 3.63 (s, 3H, OCH_3), 3.63 (s, 3H, OCH_3), 3.67-3.75 (2H, H6'), 3.70 (t, 1H, *J*=9.5 Hz, H3), 3.72-3.78 (2H, H6), 3.81 (t, 1H, *J*=9.0 Hz, H2), 3.89 (t, 1H, *J*=9.0 Hz, H4), 3.97 (m, 1H, H5), 4.04 (broad s, 1H, Hα'), 4.30 (t, 1H, *J*=6.5 Hz, Hα (near sugar residue)), 4.44 (d, 1H, *J*=8.0 Hz, H1'), 4.44 (d, 1H, *J*=14.5 Hz, NHC$\underline{H_2}$-triazole), 4.57 (d, 1H, *J*=15.5 Hz, OC$\underline{H_2}$-triazole), 5.75 (d, 1H, J=9.5 Hz, H1), 8.19 (s, 1H, C*H*, triazole)

^{13}C-NMR (125 MHz, D_2O): δ 26.0 (Cγ'), 26.9 (Cγ), 30.6 (Cβ or Cβ'), 30.8 (Cβ or Cβ'), 36.8 (NH*C*H_2-triazole), 43.0 (Cδ or Cδ'), 43.1 (Cδ or Cδ'), 51.5 (Cα'), 56.6 (Cα (near sugar residue)), 61.0 (O*C*H_3), 61.1 (O*C*H_3), 62.4 (O*C*H_3), 62.5 (O*C*H_3), 62.6 (O*C*H_3), 62.7 (O*C*H_3), 63.2 (O*C*H_3), 72.5 (C6), 73.1 (C6'), 76.1 (C5'), 78.7 (C4), 79.3 (C5), 81.4 (C4'), 84.0 (C2), 85.4 (C2'), 86.0 (C3), 87.8 (C3'), 88.9 (C1), 105.1 (C1'), 126.2 (CH of triazole), 147.5 (quaternary C of triazole). 159.4 (quaternary C of guanidino group of arginine), 159.4 (quaternary C of guanidino group of arginine), 175.8 (Cα-$\underline{C}$O-NH-), 175.9 (Cα'-$\underline{C}$O-NH-)

MALDI-TOF MS (*m/z*): calcd for $C_{34}H_{64}N_{12}O_{12}$, 832.48; found, $[M+H]^+$ = 833.63

1-[2,3,4,6-Tetra-*O*-methyl-β-D-glucopyranosyl-(1→4)-2,3,6-tri-*O*-methyl-β-D-glucopyranosyl]-4-[Fmoc-Glu(O*t*-Bu)-Glu(O*t*-Bu)-*N*-methyl]-1*H*-1,2,3-triazole (6a)

To a solution of 2,3,4,6-tetra-*O*-methyl-β-D-glucopyranosyl-(1→4)-2,3,6-tri-*O*-methyl-β-D-glucopyranosyl azide (**7a**, 25 mg, 0.054 mmol) and Fmoc-Glu(O*t*Bu)-Glu(O*t*Bu)-NH-CH_2CCH (**10**, 35 mg, 0.054 mmol) in 3 mL of methanol/dichloromethane (1/4, v/v) were added CuBr (77 mg, 0.054 mmol, 10 equiv.) and aqueous sodium ascorbate (213 mg/269 μL). The reaction mixture was stirred under nitrogen at room temperature for 2 h, after which it was purified by PTLC (eluent: 1:9 (v/v) methanol/dichloromethane) to give 1-(2,3,4,6-tetra-*O*-methyl-β-D-glucopyranosyl-(1→4)-2,3,6-tri-*O*-methyl-β-D-glucopyranosyl)-4-[*N*α-Fmoc-Glu(O*t*-Bu)-Glu(O*t*-Bu)-*N*-methyl]-1*H*-1,2,3-triazole (52 mg, 0.047 mmol, 87% yield).

^{1}H-NMR (500 MHz, $CDCl_3$): δ: 1.42 (s, 9H, CH_3 (*t*Bu)), 1.46 (s, 9H, CH_3 (*t*Bu)), 1.90-2.02 (m, 2H, Hβ), 2.02-2.20 (m, 2H, Hβ), 2.26-2.48 (m, 4H, Hγ), 2.96 (t, 1H, *J*=8.5 Hz, $H2'_{Me}$), 3.14 (t, 1H, *J*=9.0 Hz, $H3'_{Me}$), 3.15 (s, 3H, OCH_3), 3.20 (t, 1H, *J*=8.5 Hz, $H4'_{Me}$), 3.23-3.28 ($H5'_{Me}$), 3.30 (s, 3H, OCH_3), 3.39 (t, 1H, *J*=8.5 Hz, $H3_{Me}$), 3.42 (s, 3H, OCH_3), 3.54 (s, 3H, OCH_3), 3.56 (s, 3H, OCH_3), 3.62 (s, 3H, OCH_3), 3.63 (s, 3H, OCH_3), 3.54-3.58 (m, $H5_{Me}$), 3.58-3.67 (3H, $H6_{Me}$, $H6'_{Me}$), 3.64 (t, 1H, *J*=9.0 Hz, $H2_{Me}$), 3.6-3.75 (dd, 1H, *J*=4.5 Hz, *J*=11.0 Hz, $H6_{Me}$), 3.79 (t, 1H, *J*=9.5 Hz, $H4_{Me}$), 4.12 (m, 1H, Hα), 4.20 (t, 1H, *J*=4.5 Hz, C*H* (Fmoc)), 4.32 (d, 1H, *J*=8.0 Hz, $H1_{Me}$), 4.35 (broad d, 2H, *J*=7.0 Hz, CH_2 (Fmoc)), 4.43 (m, 1H, Hα), 4.54 (broad d, *J*=5.5 Hz, NH-CH_2-triazole), 5.39 (d, 1H, *J*=9.0 Hz, $H1_{Me}$), 6.07 (d, *J*=6.0 Hz, N*H*-Cα), 7.28-7.78 (8H, arom. Fmoc), 7.74 (broad s, triazole H)

826 ^{13}C-NMR (125 MHz, $CDCl_3$): δ 27.0 (triazole-CH_2-NH-Cα-*C*β-), 27.3 (*C*β-Cα-
827 NH-Fmoc), 28.0 (CH_3 (tBu)), 28.0 (CH_3 (tBu)), 31.8 (triazole-CH_2-NH-Cα-Cβ-
828 *C*γ), 31.8 (*C*γ-Cβ-Cα-NH-Fmoc), 35.1 (triazole-*C*H_2-NH-), 47.1 (CH, Fmoc),
829 53.0 (triazole-CH_2-NH-CO-*C*α-NH-), 55.3 (-CO-*C*α-NH-Fmoc), 59.0 (O*C*H_3),
830 59.3 (O*C*H_3), 60.3 (O*C*H_3), 60.3 (O*C*H_3), 60.6 (O*C*H_3), 60.7 (O*C*H_3), 60.8 (O*C*H_3),
831 67.1 (CH_2, Fmoc), 70.0 (C6), 71.1 (C6'), 74.7 (C5'), 77.1 (C4), 77.8 (C5), 79.3
832 (C4'), 81.1 (*C*$(CH_3)_3$), 81.3 (*C*$(CH_3)_3$), 81.9 (C2), 84.0 (C2'), 85.3 (C3), 86.9 (C3'),
833 87.2 (C1), 103.2 (C1'), 119.9 (arom. Fmoc), 121.6 (triazole *C*H), 125.2 (arom.
834 Fmoc), 127.1 (arom. Fmoc), 127.1 (arom. Fmoc), 127.7 (arom. Fmoc), 141.2
835 (arom. Fmoc), 141.3 (arom. Fmoc), 143.7 (arom. Fmoc), 143.9 (arom. Fmoc),
836 144.8 (O-CH_2-*C*=), 156.6 (CO Fmoc), 171.0 (Glu, triazole-CH_2-NH-*C*O-Cα-NH-),
837 171.6 (Glu, -*C*O-Cα-NH-Fmoc), 173.1 (Glu, Cδ), 173.1 (Glu, Cδ)
838 MALDI-TOF MS (*m/z*): calcd for $C_{55}H_{80}N_6O_{18}$, 1112.55; found, $[M+Na]^+$ =
839 1135.615, $[M+K]^+$ = 1151.583
840
841 **1-[2,3,4,6-Tetra-*O*-methyl-β-D-glucopyranosyl-(1→4)-2,3,6-tri-*O*-methyl-β-**
842 **D-glucopyranosyl]-4-(Glu-Glu-NH-CH_2)-1*H*-1,2,3-triazole (3a)**
843 1-[2,3,4,6-Tetra-*O*-methyl-β-D-glucopyranosyl-(1→4)-2,3,6-tri-*O*-methyl-β-D-
844 glucopyranosyl]-4-[*N*α-Fmoc-Glu(O*t*-Bu)-Glu(O*t*-Bu)-*N*-methyl]-1*H*-1,2,3-
845 triazole (**6a**, 46 mg, 0.034 mmol) was dissolved in piperidine/dichloromethane
846 (1/1, v/v, 1 mL). The reaction mixture was stirred under nitrogen at room
847 temperature for 1 h, and then concentrated to dryness. The crude product was
848 purified by PTLC (eluent: methanol/dichloromethane (15/85, v/v)) to give 1-
849 [2,3,4,6-tetra-*O*-methyl-β-D-glucopyranosyl-(1→4)-2,3,6-tri-*O*-methyl-β-D-

glucopyranosyl]-4-[Glu(O*t*-Bu)-Glu(O*t*-Bu)-*N*-methyl]-1*H*-1,2,3-triazole (24 mg, 0.016 mmol, 47% yield).

1-[2,3,4,6-Tetra-*O*-methyl-β-D-glucopyranosyl-(1→4)-2,3,6-tri-*O*-methyl-β-D-glucopyranosyl]-4-(Glu(O*t*-Bu)-Glu(O*t*-Bu)-*N*-methyl)-1*H*-1,2,3-triazole (66 mg, 0.079 mmol) was dissolved in TFA/dichloromethane (9/1, v/v, 1 mL) and stirred under nitrogen at room temperature for 4 h. The crude product was purified by gel-filtration chromatography (LH-20, eluent: methanol) to give 1-[2,3,4,6-tetra-*O*-methyl-β-D-glucopyranosyl-(1→4)-2,3,6-tri-*O*-methyl-β-D-glucopyranosyl]-4-(Glu-Glu-*N*-methyl)-1*H*-1,2,3-triazole (**3a**, 36 mg, 0.046 mmol, 58% yield).

^{1}H-NMR (500 MHz, D_2O): δ 1.9-2.1 (m, 2H, Hβ), 2.2-2.3 (m, 2H, Hβ), 2.3-2.6 (m, 4H, Hγ), 3.12 (t, 1H, *J*=8.5 Hz, H2'$_{Me}$), 3.29 (t, 1H, *J*=9.5 Hz, H4'$_{Me}$), 3.36 (t, 1H, *J*=8.5 Hz, H3'$_{Me}$), 3.36 (s, 3H, OCH_3), 3.42 (s, 3H, OCH_3), 3.43-3.48 (H5'$_{Me}$), 3.54 (s, 3H, OCH_3), 3.60 (s, 3H, OCH_3), 3.62 (s, 3H, OCH_3), 3.63 (s, 6H, OCH_3), 3.7 (H3$_{Me}$), 3.80 (t, 1H, *J*=9.5 Hz, H2$_{Me}$), 3.89 (t, 1H, *J*=9.5 Hz, H4$_{Me}$), 3.93-3.98 (m, 1H, H5$_{Me}$), 3.65-3.83 (H6'$_{Me}$, H6$_{Me}$), 3.79 (t, 1H, *J*=9.5 Hz, H4$_{Me}$), 3.86 (m, 1H, H5$_{Me}$), 4.2-4.5 (broad s, 1H, Hα), 4.34 (d, 1H, *J*=8.0 Hz, H1'$_{Me}$), 4.4-4.61 (NH-C*H*$_2$-triazole), 5.75 (broad d, 1H, *J*=7.0 Hz, H1$_{Me}$), 8.24 (broad s, triazole C*H*)

^{13}C-NMR (125 MHz, D_2O): δ 27.9 (Cβ'), 29.0 (Cβ), 31.9 (Cγ and Cγ'), 37.1 (NH*C*H$_2$-triazole), 56.1 (Cα (near sugar residue)), 59.4 (Cα'), 61.1 (O*C*H$_3$), 61.2 (O*C*H$_3$), 62.2 (O*C*H$_3$), 62.5 (O*C*H$_3$), 62.6 (O*C*H$_3$), 62.7 (O*C*H$_3$), 63.2 (O*C*H$_3$), 72.5 (C6 or C6'), 73.1 (C6 or C6'), 76.1 (C5'), 78.7 (C4), 79.4 (C5), 81.5 (C4'), 84.0 (C2), 85.5 (C2'), 86.0 (C3), 87.8 (C3'), 89.1 (C1), 105.2 (C1'), 126.6 (CH of triazole), 177.6 (Cα-CO-NH-, and Cα'-CO-NH-), 184.9 (Cγ-(CO)OH, Cγ'-(CO)OH)

MALDI-TOF MS (*m/z*): calcd for $C_{32}H_{54}N_6O_{16}$, 778.36; found, $[M+H]^+$ = 779.518, $[M+Na]^+$ = 801.530, $[M+K]^+$ = 817.504

1-(Tri-*O*-methylcellulosyl)-4-(*N*α-Fmoc-*N*ω-Pbf-L-arginine-*N*ω-Pbf-L-arginine-*N*-methyl)-1*H*-1,2,3-triazole (**5b**)

Sodium ascorbate (227 mg/287 μL, 1.15 mmol, 20 equiv., 4 M in H_2O) and $CuSO_4 \cdot 5H_2O$ (143 mg, MW = 249.69, 0.573 mmol, 10 equiv.) were added to a solution of 2-propynyl *N*α-Fmoc-*N*ω-Pbf-L-arginine-*N*ω-Pbf-L-arginine-*N*-propargylamide (**9**, 100 mg, MW = 788.8, 0.127 mmol, 2.2 equiv.) and tri-*O*-methylcellulosyl azide (**7b**, 419 mg, $M_n = 7.34 \times 10^3$, $DP_n = 35.8$, 0.0571 mmol, 1.0 equiv.) in methanol/dichloromethane (1/4, v/v, 10 mL). The reaction mixture was stirred at room temperature for 14 h under nitrogen, after which it was concentrated and passed through a silica-gel chromatography column (eluent: 20% MeOH/CH_2Cl_2) to give the crude product. The crude product was purified by gel-filtration column chromatography (LH-60, eluent: 20% MeOH/CH_2Cl_2) to give 1-(tri-*O*-methylcellulosyl)-4-(*N*α-Fmoc-*N*ω-Pbf-L-arginine-*N*ω-Pbf-L-arginine-*N*-methyl)-1*H*-1,2,3-triazole (**5b**, 420 mg, quantitative yield; GPC analysis: $M_n = 5.6 \times 10^3$, $M_w / M_n = 1.8$).

^{1}H-NMR (500 MHz, $CDCl_3$): δ: 1.44 (CH_3, Pbf), 2.07 (CH_3, Pbf), 2.47-2.56 (CH_3, Pbf), 2.92 (CH_2, Pbf), 2.96 (t, *J*=8.5 Hz, $H2_{Me}$ (internal)), 3.21 (t, 1H, *J*=9.0 Hz, $H3_{Me}$ (internal)), 3.29 (m, *J*=9.0 Hz, $H5_{Me}$ (internal)), 3.39 (s, OCH_3), 3.54 (s, OCH_3), 3.58 (s, OCH_3), 3.69 (t, *J*=9.0, $H4_{Me}$ (internal)), 3.6-3.73 (m, $H6_{Me}$ (internal)), 3.77 (m, $H6_{Me}$ (internal)), 4.34 (d, *J*=8.0 Hz, $H1_{Me}$ (internal)), 6.12 ($H1\alpha_{Me}$), 6.1-6.7, 7.24 (Fmoc), 7.35 (Fmoc), 7.57 (Fmoc), 7.62 (d, *J* = 7.0 Hz, Fmoc), 7.82.

^{13}C-NMR (125 MHz, $CDCl_3$): δ 12.5 (CH_3, Pbf), 17.9 (CH_3, Pbf), 19.3 (CH_3, Pbf), 25.5 (Cγ), 28.6 (CH_3, Pbf), 40.9 (Cδ), 43.2 ($\underline{C}H_2$, Pbf), 47.0 (<u>C</u>H, Fmoc), 59.1 (O*C*H_3), 60.3 (O*C*H_3), 60.5 (O*C*H_3), 67.3 ($\underline{C}H_2$, Fmoc), 70.3 (C6), 74.8 (C5), 77.4 (C4), 83.5 (C2), 85.0 (C3), 86.4 (CH, Fmoc), 103.1 (C1), 117.6 (arom. Pbf), 119.9 (arom. Fmoc), 124.7 (arom. Pbf), 125.2 (arom. Fmoc), 127.1 (arom. Fmoc), 127.7 (arom. Fmoc), 132.3 (arom. Pbf), 132.7 (arom. Pbf), 138.3 (arom. Pbf), 141.1 (arom. Fmoc), 143.7 (arom. Fmoc), 156.4 (arom. Pbf), 158.8 (-O-<u>C</u> arom. Pbf)

FT-IR (KBr): 3442, 2930, 2836, 1722, 1663, 1622, 1551, 1454, 1375, 1310, 1125, 1184, 951, 853, 812, 785, 761, 741 (Fmoc), 700, 662, 567 (Pbf, -SO_2NH-) cm^{-1}

1-(Tri-*O*-methylcellulosyl)-4-(L-arginine-L-arginine-*N*-methyl)-1*H*-1,2,3-triazole (2b)

1-(Tri-*O*-methylcellulosyl)-4-(*N*α-Fmoc-*N*ω-Pbf-L-arginine-*N*ω-Pbf-L-arginine-*N*-methyl)-1*H*-1,2,3-triazole (**5b**, 293 mg) was dissolved in piperidine/dichloromethane (1/1, v/v, 4 mL). The reaction mixture was stirred at room temperature for 4 h under nitrogen, after which it was concentrated and purified by gel-filtration column chromatography (LH-60, eluent: 20% MeOH/CH_2Cl_2) to give 1-(tri-*O*-methylcellulosyl)-4-(*N*ω-Pbf-L-arginine-*N*ω-Pbf-L-arginine-*N*-methyl)-1*H*-1,2,3-triazole (260 mg, 89% yield; GPC analysis: M_n = 6.7×10^3, M_w / M_n = 1.7).

1-(Tri-*O*-methylcellulosyl)-4-(*N*ω-Pbf-L-arginine-*N*ω-Pbf-L-arginine-*N*-methyl)-1*H*-1,2,3-triazole (244 mg) was dissolved in trifluoroacetic acid/distilled water (1/4, v/v, 2 mL) and stirred at 37 °C for 4 h under nitrogen. The mixture

was concentrated, purified by gel-filtration column chromatography (LH-60, eluent: 20% MeOH/CH_2Cl_2), and further purified by PTLC (eluent: 10% MeOH/CH_2Cl_2). The purified 1-(tri-*O*-methyl-cellulosyl)-4-(L-arginine-L-arginine-*N*-methyl)-1*H*-1,2,3-triazole was dispersed in water. Water-soluble component was collected by removal of the water-insoluble component by filtration through cotton wool, which was then concentrated to give 1-(tri-*O*-methylcellulosyl)-4-(L-arginine-L-arginine-*N*-methyl)-1*H*-1,2,3-triazole (**2b**, 186 mg, 76% yield, GPC analysis: $M_n = 6.0 \times 10^3$, $M_w / M_n = 1.6$).

^{1}H-NMR (500 MHz, D_2O): δ 1.5-2.0 (m, Hγ and Hγ', Hβ, Hβ'), 3.13 (t, *J*= 8.5 Hz, $H2_{Me}$), 3.40 (s, OMe), 3.45 (t, *J* = 9.5 Hz, $H3_{Me}$), 3.56 (s, OMe), 3.58 (s, OMe), 3.55-3.60 ($H5_{Me}$), 3.68-3.80 ($H4_{Me}$, $H6_{Me}$), 4.42 (d, *J* = 7.5 Hz, $H1_{Me}$), 4.65 (d, *J* = 8.0 Hz), 4.99 (d, *J* = 3.5 Hz), 5.40 (d, *J* = 3.5 Hz), 5.62 (broad s), 8.42 (s, C*H*, triazole)

FT-IR (KBr): 3446, 2922, 2836, 1624, 1456, 1375, 1314, 1125, 1078, 947, 768, 702, 662, 606, 581, 538, 488 cm^{-1}

1-(Tri-*O*-methyl-cellulosyl)-4-[Fmoc-Glu(O*t*-Bu)-Glu(O*t*-Bu)-*N*-methyl]-1*H*-1,2,3-triazole (**6b**)

Sodium ascorbate (109 mg/137 μL, 0.55 mmol, 20 equiv., 4 M in H_2O) and $CuSO_4 \cdot 5H_2O$ (68 mg, MW = 249.69, 0.27 mmol, 10 equiv.) were added to a solution of *N*α-Fmoc-Glu(O*t*-Bu)-Glu(O*t*-Bu)-*N*-propargylamide (**10**, 53 mg, MW = 647.77, 0.082 mmol, 3.0 equiv.) and tri-*O*-methylcellulosyl azide (**7b**, 200 mg, $M_n = 7.34 \times 10^3$, $DP_n = 35.8$, 0.027 mmol, 1.0 equiv.) in methanol/dichloromethane (1/4, v/v, 5 mL). The reaction mixture was stirred at room temperature for 14 h under nitrogen, after which it was concentrated and

passed through a silica-gel chromatography column (eluent: 20% MeOH/CH_2Cl_2). The crude product was purified by gel-filtration column chromatography (LH-60, eluent: 20% MeOH/CH_2Cl_2), and then by PTLC (eluent: 10% MeOH/CH_2Cl_2) to give 1-(tri-*O*-methylcellulosyl)-4-[Fmoc-Glu(O*t*-Bu)-Glu(O*t*-Bu)-*N*-methyl]-1*H*-1,2,3-triazole (186 mg, 93% yield, GPC analysis: $M_n = 7.4 \times 10^3$, $M_w / M_n = 1.6$).

^{1}H-NMR (500 MHz, $CDCl_3$): δ 1.43 (s, CH_3 (*t*Bu)), 1.47 (s, CH_3 (*t*Bu)), 2.0-2.2 (m, 4H, Hβ), 2.25-2.450 (m, 4H, Hγ), 2.96 (t, *J*= 8.5 Hz, $H2_{Me}$), 3.22 (t, *J*= 9.0 Hz, $H3_{Me}$), 3.29 (m, $H5_{Me}$), 3.39 (s, OMe), 3.54 (s, OMe), 3.59 (s, OMe), 3.64-3.74 ($H4_{Me}$), 3.64-3.82 ($H6_{Me}$), 4.1-4.2 (1H, Hα), 4.25-4.35 (2H, C*H*$_2$ (Fmoc)), 4.35 (d, *J*= 7.5 Hz, $H1_{Me}$), 7.32 (t, *J*= 7.5 Hz, arom., Fmoc), 7.40 (t, *J*= 7.5 Hz, arom., Fmoc), 7.62 (broad d, *J*= 7.0 Hz, arom., Fmoc), 7.76 (d, *J*= 7.5 Hz, arom., Fmoc)

^{13}C-NMR (125 MHz, $CDCl_3$): δ 28.0 (CH_3 (tBu)), 28.0 (CH_3 (tBu)), 31.9 (triazole-CH_2-NH-Cα-Cβ-*C*γ), 35.2 (triazole-*C*H_2-NH-), 47.1 (CH, Fmoc), 59.1 (O*C*H_3), 59.6, 60.1, 60.3 (O*C*H_3), 60.4, 60.5 (O*C*H_3), 60.8, 67.2 (CH_2, Fmoc), 70.3 (C6), 72.2, 73.2, 73.2, 74.9 (C5), 77.4 (C4), 81.2 (*C*$(CH_3)_3$), 83.5 (C2), 85.0 (C3), 86.1, 103.1 (C1), 120.0 (arom. Fmoc), 125.1 (arom. Fmoc), 127.1 (arom. Fmoc), 127.7 (arom. Fmoc), 141.3 (arom. Fmoc), 143.8 (arom. Fmoc), 144.4 (arom. Fmoc)

FT-IR (KBr): 3430, 2932, 2904, 2836, 1728, 1672, 1514 (*t*Bu), 1454, 1373, 1312, 1125, 1084, 1059, 951, 889, 851, 762, 743 (Fmoc), 704, 656, 615, 577 cm^{-1}

1-(Tri-*O*-methyl-cellulosyl)-4-(Glu-Glu-*N*-methyl)-1H-1,2,3-triazole (3b)

1-(Tri-*O*-methyl-cellulosyl)-4-[Fmoc-Glu(O*t*-Bu)-Glu(O*t*-Bu)-*N*-methyl]-1*H*-1,2,3-triazole (161 mg) was dissolved in piperidine/dichloromethane (1/1, v/v, 2 mL). The reaction mixture was stirred at room temperature for 4 h under nitrogen,

after which it was concentrated and purified by gel-filtration column chromatography (LH-60, eluent: 20% MeOH/CH_2Cl_2), and then by PTLC (eluent: 10% MeOH/CH_2Cl_2) to give 1-(tri-*O*-methylcellulosyl)-4-[Glu(O*t*-Bu)-Glu(O*t*-Bu)-*N*-methyl]-1H-1,2,3-triazole (136 mg, 84% yield; GPC analysis: M_n = 8.0×10^3, $M_w / M_n = 1.6$).

1-(Tri-*O*-methylcellulosyl)-4-[Glu(O*t*-Bu)-Glu(O*t*-Bu)-*N*-methyl]-1H-1,2,3-triazole (124 mg) was dissolved in trifluoroacetic acid/distilled water (9/1, v/v, 1 mL). The reaction mixture was stirred at room temperature for 4 h under nitrogen atmosphere, concentrated, and then purified by gel-filtration column chromatography (LH-60, eluent: 20% MeOH/CH_2Cl_2), and further purified by PTLC) eluent: 10% MeOH/CH_2Cl_2). The water-soluble component was collected by removal of the water-insoluble component by filtration, and concentrated to give 1-(tri-*O*-methylcellulosyl)-4-(Glu-Glu-*N*-methyl)-1*H*-1,2,3-triazole (**3b**, 64 mg, 52% yield; GPC analysis: $M_n = 7.0 \times 10^3$, M_w / M_n =1.6).

^{1}H-NMR (500 MHz, D_2O): δ 3.14 (t, J = 9.0 Hz, $H2_{Me}$), 3.40 (s, OMe), 3.45 (t, J = 9.0 Hz, $H3_{Me}$), 3.57 (s, OMe), 3.58 (s, OMe), 3.57-3.62 ($H5_{Me}$), 3.60-3.82 ($H4_{Me}$, $H6_{Me}$), 4.43 (d, J = 8.0 Hz, $H1_{Me}$), 4.48 (d, 5.40 (d, J = 3.0 Hz), J = 3.5 Hz), 5.43 (broad s), 8.43 (s, triazole C*H*)

FT-IR (KBr): 3460, 2928, 2836, 1732, 1626, 1458, 1377, 1310, 1126, 1084, 1061, 945, 800, 704, 664, 571, 486 cm^{-1}

Characterization

General

^{1}H- and ^{13}C-NMR spectra were recorded on a Varian 500 NMR (500 MHz) or Varian INOVA300 (300 MHz) spectrometer in chloroform-*d* with tetramethylsilane as the internal standard, or in deuterium oxide with 3-

(trimethylsilyl)-1-propanesulfonic acid sodium salt as the external standard. Chemical shifts (δ) and coupling constants (J) are given in ppm and Hz, respectively. Matrix-assisted laser-desorption/ionization time-of-flight mass spectrometry (MALDI-TOF MS) was performed on a Bruker MALDI-TOF Autoflex III mass spectrometer in positive ion and reflector or linear modes. A smartbeam laser was used for ionization. All spectra were acquired in linear mode and calibrated externally. 2,5-Dihydroxybenzoic acid was used as the matrix in MALDI-TOF MS experiments. Shimadzu components, namely the liquid chromatography injector (LC-10ATvp), column oven (CTO-10Avp), ultraviolet-visible detector (SPD-10Avp), refractive index detector (RID-10A), communication bus module (CBM-10A), and LC workstation (CLASS-LC10), were used for HPLC separations, with Shodex columns (KF802, KF802.5, and KF805). Number- and weight-averaged molecular weights (M_n, M_w) and polydispersity indices (M_w/M_n) were determined using polystyrene standards (Shodex). A flow rate of 1 mL/min at 40 °C was chosen, and chloroform was used as the eluent.

Differential scanning calorimetry (DSC)

DSC thermograms were recorded on a DSC823^e instrument (Mettler Toledo, Zurich, Switzerland) with an HSS7 sensor under nitrogen during (0 → 90 → 0 °C) heating/cooling cycles, with heating and cooling rates of 3.5 °C/min. Each temperature cycle was repeated three times in order to ensure reproducibility. Sample concentrations of 2.0 wt% were used in DSC experiments.

Dynamic light scattering (DLS) experiments

DLS experiments were performed with an ELS-Z zeta-potential and particle-size analyzer (Otsuka Electronics Co., Ltd, Osaka, Japan) and conducted in the

10–90 °C temperature range. Sample solutions were maintained at the required temperature for 5 min prior to each experiment. Sample concentrations of 0.2 wt% were used in these experiments.

Surface-tension measurements

Surface tensions were measured with a CBVP-A3 surface tensiometer (Kyowa Interface Science, Co. Ltd., Tokyo, Japan) at 23 °C using the Wilhelmy method. A Teflon cell containing 700 μL of the required solution was used in these experiments. Surface tensions gradually decreased with time, and stable values were recorded after 30 min.

Scanning electron microscopy (SEM) and transmission electron microscopy (TEM)

The three hydrogels from aqueous solutions containing compounds **1b**, **2b**, and **3b** were frozen in liquid nitrogen, lyophilized, and cut with a razor blade. The cut surfaces of the hydrogels were sputter-coated with gold with an ion-coater (JFC-1100E, JEOL, Tokyo, Japan) and examined by scanning electron microscopy (SEM, JSM-6060, JEOL) at an accelerator voltage of 5 kV.

A drop of an aqueous dispersion of compound **2b** was mounted on a copper grid with an elastic carbon-support film (Oken Shoji, Tokyo, Japan) and examined by transmission electron microscopy (TEM, JEM1400, JEOL) at an accelerator voltage of 100 kV after negative staining with uranyl acetate.

Release of model drugs from the thermoresponsive hydrogels

Compounds **2b** and **3b** (2 or 4 mg) were respectively added to glass vials containing solutions of diclofenac sodium (DFNa) or imipramine hydrochloride (IMC) (0.025 wt%) in PBS (100 μL), and the compounds were dissolved at about 0 °C. The glass vial was then heated at 37 °C for 10 min while left to stand. After

a hydrogel had formed, a fresh PBS solution (500 μL), which had been pre-heated to 37 °C, was carefully poured onto the hydrogel surface. The glass vial was shaken at 60 rpm in a water-bath shaker (Eyela NTS-4000, Tokyo Rikakikai Co., Ltd.). The aqueous layer (500 μL) was then collected and filtered through a membrane filter (pore size: 0.45 μm). The UV absorbance of the aqueous solution was recorded at 260 nm in a 96-well microplate using a SpectraMax Plus 384 Microplate Reader (Molecular Devices). The amount of released drug was evaluated from the UV absorbance.

Cytotoxicity assays

Compounds **1b**, **2b**, and **3b** were dispersed in PBS at a concentration of 20 mg/mL and serially diluted by factors of two in a 96-well flat-bottomed plate (50 μL/well (Corning Inc., Corning, NY). The human histocytoma U937 cell line was suspended in complete RPMI1640 medium at 1×10^4 cells/mL and the cell suspension was added to the 96-well flat bottom plate (5×10^2 cells/50 μl/well). The plate was incubated at 37 °C in a 5%-CO_2 atmosphere for 4 d. The plate was allowed to stand at room temperature for 30 min, after which 100 μL of CellTiter-Glo Luminescent Cell Viability Assay reagent (Promega Corp., Madison, WI) was added to each well. After thorough mixing, the contents of each well were transferred into an Optiplate™-96 multi-well plate (Perkin Elmer, Waltham, MA). Cell viability was determined by measuring luminescence with an ARVO™ SX Delfia 1420 Multilabel Counter (Perkin Elmer Life and Analytical Sciences, Shelton, CT).

Acknowledgements This work was supported in part by JSPS Grants-in-Aid for Scientific Research (B) nos. 24380092 and 15H04531.

References

Aagren JKM, Billing JF, Grundberg HE, Nilsson UJ (2006) Synthesis of a chiral and fluorescent sugar-based macrocycle by 1,3-dipolar cycloaddition Synthesis:3141-3145 doi:10.1055/s-2006-942503

Akiyoshi K, Kohara M, Ito K, Kitamura S, Sunamoto J (1999) Enzymic synthesis and characterization of amphiphilic block copolymers of poly(ethylene oxide) and amylose Macromol Rapid Commun 20:112-115 doi:10.1002/(SICI)1521-3927(19990301)20:3<112::AID-MARC112>3.0.CO;2-Q

Baumann MD, Kang CE, Stanwick JC, Wang Y, Kim H, Lapitsky Y, Shoichet MS (2009) An injectable drug delivery platform for sustained combination therapy J Controlled Release 138:205-213 doi:10.1016/j.jconrel.2009.05.009

Bodvik R et al. (2010) Aggregation and network formation of aqueous methylcellulose and hydroxypropylmethylcellulose solutions Colloids Surf, A 354:162-171 doi:10.1016/j.colsurfa.2009.09.040

Bonduelle C, Lecommandoux S (2013) Synthetic Glycopolypeptides as Biomimetic Analogues of Natural Glycoproteins Biomacromolecules 14:2973-2983 doi:10.1021/bm4008088

Breitenbach BB, Schmid I, Wich PR (2017) Amphiphilic Polysaccharide Block Copolymers for pH-Responsive Micellar Nanoparticles Biomacromolecules 18:2839-2848 doi:10.1021/acs.biomac.7b00771

Dax D, Xu C, Langvik O, Hemming J, Backman P, Willfoer S (2013) Synthesis of SET-LRP-induced galactoglucomannan-diblock copolymers J Polym Sci, Part A: Polym Chem 51:5100-5110 doi:10.1002/pola.26942

de Medeiros Modolon S, Otsuka I, Fort S, Minatti E, Borsali R, Halila S (2012) Sweet Block Copolymer Nanoparticles: Preparation and Self-Assembly of Fully Oligosaccharide-Based Amphiphile Biomacromolecules 13:1129-1135 doi:10.1021/bm3000138

Desbrieres J, Hirrien M, Rinaudo M (1998) A calorimetric study of methylcellulose gelation Carbohydr Polym 37:145-152

Du X, Zhou J, Shi J, Xu B (2015) Supramolecular Hydrogelators and Hydrogels: From Soft Matter to Molecular Biomaterials Chemical Reviews 115:13165-13307 doi:10.1021/acs.chemrev.5b00299

Fajardo AR, Guerry A, Britta EA, Nakamura CV, Muniz EC, Borsali R, Halila S (2014) Sulfated Glycosaminoglycan-Based Block Copolymer: Preparation of Biocompatible Chondroitin Sulfate-b-poly(lactic acid) Micelles Biomacromolecules 15:2691-2700 doi:10.1021/bm5005355

Fundueanu G, Constantin M, Ascenzi P (2009) Poly(N-isopropylacrylamide-co-acrylamide) cross-linked thermoresponsive microspheres obtained from preformed polymers: influence of the physico-chemical characteristics of drugs on their release profiles Acta Biomater 5:363-373 doi:10.1016/j.actbio.2008.07.011

Heymann E (1935) Studies on sol-gel transitions. 1. The inverse sol-gel transformation of methylcellulose in water Trans Faraday Soc 31:846

Hung C-C et al. (2017) Conception of Stretchable Resistive Memory Devices Based on Nanostructure-Controlled Carbohydrate-block-Polyisoprene Block Copolymers Adv Funct Mater 27:n/a doi:10.1002/adfm.201606161

Kamitakahara H, Baba A, Yoshinaga A, Suhara R, Takano T (2014) Synthesis and crystallization-induced microphase separation of cellulose triacetate-block-poly(γ -benzyl-L-glutamate) Cellulose (Dordrecht, Neth) 21:3323-3338 doi:10.1007/s10570-014-0383-3

Kamitakahara H, Funakoshi T, Nakai S, Takano T, Nakatsubo F (2009a) Syntheses of 6-O-ethyl/methyl-celluloses via ring-opening copolymerization of 3-O-benzyl-6-O-ethyl/methyl-alpha-d-glucopyranose 1,2,4-orthopivalates and their structure-property relationships Cellulose 16:1179-1185 doi:Doi 10.1007/S10570-009-9339-4

Kamitakahara H, Funakoshi T, Takano T, Nakatsubo F (2009b) Syntheses of 2,6-O-alkyl celluloses: Influence of methyl and ethyl groups regioselectively introduced at O-2 and O-6 positions on their solubility Cellulose 16:1167-1178

Kamitakahara H, Koschella A, Mikawa Y, Nakatsubo F, Heinze T, Klemm D (2008a) Syntheses and comparison of 2,6-di-O-methyl celluloses from natural and synthetic celluloses Macromolecular Bioscience 8:690-700

Kamitakahara H, Murata-Hirai K, Tanaka Y (2012) Synthesis of blockwise alkylated tetrasaccharide-organic quantum dot complexes and their utilization for live cell labeling with low cytotoxicity Cellulose 19:171-187 doi:Doi 10.1007/S10570-011-9619-7

Kamitakahara H, Nakatsubo F (2010) ABA- and BAB-triblock cooligomers of tri-O-methylated and unmodified cello-oligosaccharides: syntheses and structure-solubility relationship Cellulose 17:173-186 doi:Doi 10.1007/S10570-009-9348-3

Kamitakahara H, Nakatsubo F, Klemm D (2006) Block co-oligomers of tri-O-methylated and unmodified cello-oligosaccharides as model compounds for methylcellulose and its dissolution/gelation behavior Cellulose 13:375-392

Kamitakahara H, Nakatsubo F, Klemm D (2007) New class of carbohydrate-based nonionic surfactants: diblock co-oligomers of tri-O-methylated and unmodified cello-oligosaccharides Cellulose 14:513-528

Kamitakahara H, Nakatsubo F, Klemm D (2009c) Synthesis of methylated cello-oligosaccharides: synthesis strategy for block-wise methylated cello-oligosaccharides ACS Symp Ser 1017:199-211 doi:10.1021/bk-2009-1017.ch011

Kamitakahara H, Suhara R, Yamagami M, Kawano H, Okanishi R, Asahi T, Takano T (2016) A versatile pathway to end-functionalized cellulose ethers for click chemistry applications Carbohydr Polym 151:88-95 doi:10.1016/j.carbpol.2016.05.016

Kamitakahara H, Yoshinaga A, Aono H, Nakatsubo F, Klemm D, Burchard W (2008b) New approach to unravel the structure-property relationship of methylcellulose. Self-assembly of amphiphilic block-like methylated cello-oligosaccharides Cellulose 15:797-801 doi:10.1007/s10570-008-9232-6

Karakawa M, Mikawa Y, Kamitakahara H, Nakatsubo F (2002) Preparations of regioselectively methylated cellulose acetates and their H-1 and C-13 NMR spectroscopic analyses J Polym Sci Pol Chem 40:4167-4179

Kato T, Yokoyama M, Takahashi A (1978) Melting temperatures of thermally reversible gels Colloid Polym Sci 256:15-21

Kunishima M, Kawachi C, Iwasaki F, Terao K, Tani S (1999a) Synthesis and characterization of 4-(4,6-dimethoxy-1,3,5-triazin-2-yl)-4-methylmorpholinium chloride Tetrahedron Lett 40:5327-5330 doi:10.1016/S0040-4039(99)00968-5

Kunishima M, Kawachi C, Morita J, Terao K, Iwasaki F, Tani S (1999b) 4-(4,6-Dimethoxy-1,3,5-triazin-2-yl)-4-methylmorpholinium chloride: an efficient condensing agent leading to the formation of amides and esters Tetrahedron 55:13159-13170 doi:10.1016/S0040-4020(99)00809-1

Liu J-Y, Zhang L-M (2007) Preparation of a polysaccharide-polyester diblock copolymer and its micellar characteristics Carbohydr Polym 69:196-201 doi:10.1016/j.carbpol.2006.09.009

Loos K, Müller AHE (2002) New Routes to the Synthesis of Amylose-block-polystyrene Rod−Coil Block Copolymers Biomacromolecules 3:368-373 doi:10.1021/bm0156330

Lott JR, McAllister JW, Arvidson SA, Bates FS, Lodge TP (2013a) Fibrillar Structure of Methylcellulose Hydrogels Biomacromolecules 14:2484-2488 doi:10.1021/bm400694r

Lott JR, McAllister JW, Wasbrough M, Sammler RL, Bates FS, Lodge TP (2013b) Fibrillar Structure in Aqueous Methylcellulose Solutions and Gels Macromolecules (Washington, DC, U S) 46:9760-9771 doi:10.1021/ma4021642

Morelli P, Matile S (2017) Sidechain Engineering in Cell-Penetrating Poly(disulfide)s Helv Chim Acta 100:e1600370 doi:10.1002/hlca.201600370

Nakagawa A, Fenn D, Koschella A, Heinze T, Kamitakahara H (2011a) Physical Properties of Diblock Methylcellulose Derivatives with Regioselective Functionalization Patterns: First Direct Evidence that a Sequence of 2,3,6-Tri-O-methyl-glucopyranosyl Units Causes Thermoreversible Gelation of Methylcellulose Journal of Polymer Science Part B-Polymer Physics 49:1539-1546 doi:Doi 10.1002/Polb.22343

Nakagawa A, Fenn D, Koschella A, Heinze T, Kamitakahara H (2011b) Synthesis of Diblock Methylcellulose Derivatives with Regioselective Functionalization Patterns J Polym Sci Pol Chem 49:4964-4976 doi:Doi 10.1002/Pola.24952

Nakagawa A, Ishizu C, Sarbova V, Koschella A, Takano T, Heinze T, Kamitakahara H (2012a) 2-O-Methyl- and 3,6-Di-O-methyl-cellulose from Natural Cellulose: Synthesis and Structure Characterization Biomacromolecules 13:2760-2768 doi:Doi 10.1021/Bm300754u

Nakagawa A, Kamitakahara H, Takano T (2011c) Synthesis of blockwise alkylated (1-->4) linked trisaccharides as surfactants: influence of configuration of anomeric position on their surface activities Carbohydr Res 346:1671-1683 doi:10.1016/j.carres.2011.04.034

Nakagawa A, Kamitakahara H, Takano T (2012b) Synthesis and thermoreversible gelation of diblock methylcellulose analogues via Huisgen 1,3-dipolar cycloaddition Cellulose 19:1315-1326 doi:Doi 10.1007/S10570-012-9703-7

Nakagawa A, Steiniger F, Richter W, Koschella A, Heinze T, Kamitakahara H (2012c) Thermoresponsive Hydrogel of Diblock Methylcellulose: Formation of Ribbonlike Supramolecular Nanostructures by Self-Assembly Langmuir 28:12609-12618

Otsuka I, Osaka M, Sakai Y, Travelet C, Putaux J-L, Borsali R (2013) Self-Assembly of Maltoheptaose-block-Polystyrene into Micellar Nanoparticles and Encapsulation of Gold Nanoparticles Langmuir 29:15224-15230 doi:10.1021/la403941v

Otsuka I, Travelet C, Halila S, Fort S, Pignot-Paintrand I, Narumi A, Borsali R (2012) Thermoresponsive Self-Assemblies of Cyclic and Branched Oligosaccharide-block-poly(N-isopropylacrylamide) Diblock Copolymers into Nanoparticles Biomacromolecules 13:1458-1465 doi:10.1021/bm300167e

Parker J, Mitrousis N, Shoichet MS (2016) Hydrogel for Simultaneous Tunable Growth Factor Delivery and Enhanced Viability of Encapsulated Cells in Vitro Biomacromolecules 17:476-484 doi:10.1021/acs.biomac.5b01366

Rees DA (1972) Polysaccharide gels, A molecular view Chem & Ind (London) 19:630-636

Sakai-Otsuka Y, Zaioncz S, Otsuka I, Halila S, Rannou P, Borsali R (2017) Self-Assembly of Carbohydrate-block-Poly(3-hexylthiophene) Diblock Copolymers into Sub-10 nm Scale Lamellar Structures Macromolecules 50:3365-3376 doi:10.1021/acs.macromol.7b00118

Savage AB (1957) Temperature-Viscosity Relationships for Water-Soluble Cellulose Ethers Ind Eng Chem 49:99

Schamann M, Schafer HJ (2003) TEMPO-mediated anodic oxidation of methyl glycosides and 1-methyl and 1-azido disaccharides Eur J Org Chem:351-358 doi:10.1002/ejoc.200390041

Togashi D, Otsuka I, Borsali R, Takeda K, Enomoto K, Kawaguchi S, Narumi A (2014) Maltopentaose-Conjugated CTA for RAFT Polymerization Generating Nanostructured Bioresource-Block Copolymer Biomacromolecules 15:4509-4519 doi:10.1021/bm501314f

Yagi S, Kasuya N, Fukuda K (2010) Synthesis and characterization of cellulose-b-polystyrene Polym J (Tokyo, Jpn) 42:342-348 doi:10.1038/pj.2009.342

Yamagami M, Kamitakahara H, Yoshinaga A, Takano T (2018) Thermo-reversible supramolecular hydrogels of trehalose-type diblock methylcellulose analogues Carbohydr Polym 183:110-122 doi:10.1016/j.carbpol.2017.12.006

Yang HW, Yi JW, Bang E-K, Jeon EM, Kim BH (2011) Cationic nucleolipids as efficient siRNA carriers Org Biomol Chem 9:291-296 doi:10.1039/C0OB00580K

Ying LQ, Gervay-Hague J (2003) General methods for the synthesis of glycopyranosyluronic acid azides Carbohyd Res 338:835-841 doi:10.1016/S0008-6215(03)00042-9

Yu G-J, Chen X-Y, Mao S-Z, Liu M-L, Du Y-R (2017) Hydrophobic terminal group of surfactant initiating micellization as revealed by 1H NMR spectroscopy Chin Chem Lett 28:1413-1416 doi:10.1016/j.cclet.2017.04.013